Online Supplement

# Learning rules of engagement for social exchange within and between groups

Michael Rojek-Giffin[1*], Maël Lebreton[2,3*,#], Jean Daunizeau[4,5], Andrea Fariña[1], Jörg Gross[1,6], and Carsten K.W. De Dreu[1,7,#]

[1] Institute for Psychology, Leiden University, the Netherlands

[2] Paris-Jourdan Sciences Economiques UMR8545, Paris School of Economics, France

[3] Swiss Centre for Affective Sciences, Faculty of Psychology and Educational Sciences, Université de Genève, Switzerland

[4] Sorbonne Université, France

[5] Paris Brain Institute (ICM), Pitié-Salpêtrière Hospital, 75013, Paris, France

[6] Institute of Psychology, University of Zurich, Switzerland

[7] CREED, University of Amsterdam, the Netherlands

[*] Indicates shared first authorship

[#] Corresponding authors at Leiden University, PO 9555, 2300 RB Leiden, the Netherlands; email: c.k.w.de.dreu@fsw.leidenuniv.nl and Paris School of Economics, Paris, France; email: mael.lebreton@psemail.eu

**Content**

## I. Behavioral Experiments

**I.1 Research Ethics and Sample**. Data were collected in five independent samples: Experiment 1: *N* = 210; Experiment 2: *N* = 50; Experiment 3: *N* = 162; Experiment 4: *N* = 169; Experiment 5: *N* = 49. All experiments received ethics approval from Leiden University (CEP17-0829/274, CEP17-1012/341, CEP19-0617/350/NL43120.058.13, 2020-07-07-C.K.W.deDreu-V3-2504, and 2020-11-17-C.K.W.de Dreu-V1-2767). Participants were recruited from the subject pool at Leiden University (Experiments 1,2,5) or from the online experimental tool Prolific (Experiments 3,4), provided written informed consent and were debriefed and paid for participation. Experiments were incentivized and did not involve deception. Individual anonymity was guaranteed throughout and earnings were paid in private.

Experiments were pre-registered prior to data collection and can be found at the following links: https://osf.io/vcweq; https://osf.io/wreaq; https://osf.io/qv5g9; https://osf.io/3fwnt. Important to note that in Experiment 5, 50 participants were invited to participate, however due to a technical failure of the scanner data was lost for one participant. The final sample for this experiment was thus 49 participants.

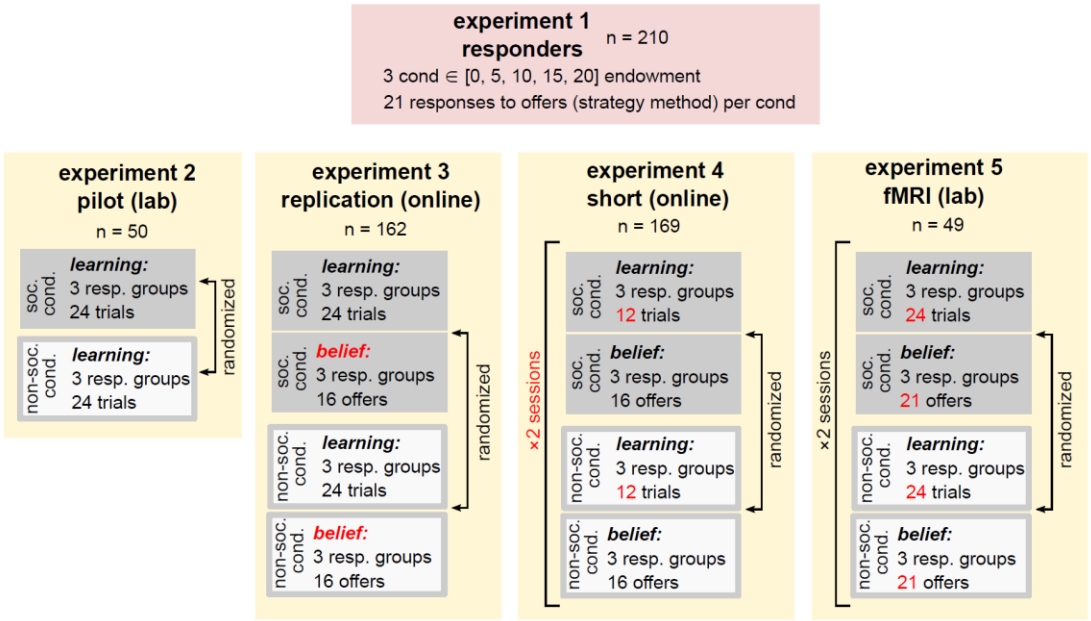


**Figure S1. Study design.** Data was collected across five independent experiments. In Experiment 1, participants provided ultimatum game responses for each possible offer in five different conditions in which they were given five different starting endowments. This resulted in different distributions of acceptance frequencies which were used as feedback for Experiments 2-5. Experiments 2-5 all consisted of proposers learning the acceptance thresholds of the responder groups collected in Experiment 1. All changes in experiment design (from left to right) are denoted with red. In Experiment 2, participants completed 1 session of social and 1 session of non-social learning (24 trials each). In Experiment 3, we introduced the belief estimation task (restricted to offers between 0 and 15) after each learning session. In Experiment 4, participants completed 2 sessions of both social and non-social learning (12 trials each) followed by the belief estimation task (restricted to offers between 0 and 15). Finally, in Experiment 5, participants

completed 2 sessions of both social and non-social learning (24 trials each) followed by the belief estimation task (with all possible offers).

**I.2 Creating Different Responder Groups**. To obtain the responder populations against which our proposers played, we first invited 210 participants to play the Ultimatum Game (UG) as responders using the strategy method (Experiment 1). Responders played in five different conditions consisting of starting endowments with different amounts of monetary units (MU): 0MU, 5MU, 10MU, 15MU or 20MU (**Fig. S1**). These different starting endowments given to the responders resulted in different amounts of money being at stake on any given trial. For example, when the responder received a starting endowment of 0MU, all the money at stake on that trial would be in the hands of the proposer. Therefore, a 50/50 division of the total amount at stake on such a trial would be 10MU from the proposer. However, on a trial in which the responder received a starting endowment of 10MU, the total amount at stake would now be the proposer's starting endowment (20MU) plus the responder's starting endowment (10MU), totaling 30MU at stake altogether, and making a 50/50 division equal to 5MU instead of 10MU. On trials in which the responder received a starting endowment of 20MU, there was 40MU at stake altogether, and an offer of 0MU resulted in a 50/50 division. By manipulating the starting endowment, we were able to shift acceptance thresholds across groups, allowing us to 'create' different populations with differing underlying expectations (or fairness norms), akin to different conventions or norms about fairness and pro-sociality found in different natural groups (1–4).

Responders were asked if they would accept all offers between 0 and 20 (**Fig S2A**) and their answers were then pooled and summed to obtain the frequency with which each offer was accepted in a given condition. The condition in which responders received a starting endowment of 0MU exhibited a distribution commonly found in the Ultimatum Game in Western samples, with offers of 10MU being accepted in most cases, but offers below 10MU being frequently rejected. More importantly, the conditions in which responders received initial starting endowments resulted in responders accepting lower offers. The resulting distributions of this manipulation acted as the populations against which our proposer played in experiment 2-5. Specifically, using Matlab's "fit" function, we fit logistic functions over the resulting distributions of this manipulation in order to obtain the acceptance threshold of the respective population (see **Fig 1**, Main Text). In order to obtain functions that adequately described the most relevant portion of the offer space (i.e., offers between 0 and 10, as offers over 10 are seldomly made by proposers), we constrained our function's slopes to be positive. Specifically, we determined whether the acceptance probability of each successive offer was increasing as the offer amount increased. If for any successive offer, the acceptance probability decreased, we forced the sigmoid to continue increasing. If we did not employ this procedure, the logistic functions used to summarize the acceptance data would become inaccurate for offers between

0 and 10 due to the model's attempt to fit to declining values above 10. We selected three of the resulting functions (endowment 0MU, 10MU, 20MU) to provide feedback to our proposers in Experiment 2-5 (also see **Fig 1**, Main Text).

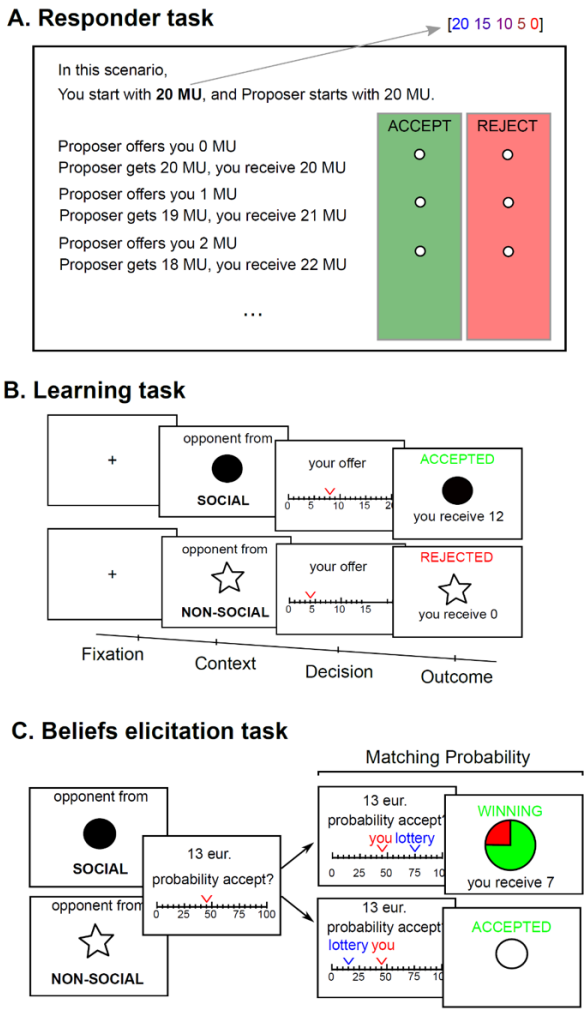


**Figure S2. Responder task. A.** In Experiment 1, participants provided ultimatum game responses for each possible offer in five different conditions in which they were given five different starting endowments. This resulted in different distributions of acceptance frequencies which were used as feedback for Experiments 2-5. **B.** In Experiments 2-5, participants made offers to different responders who were grouped based on their starting endowment. Each responder group was demarcated by a neutral shape. **C.** Participants in Experiments 3-5 completed a fully incentivized probability matching task in which they provided estimates for the likelihood of acceptance for each possible offer separately for each responder group.

**I.3 Ultimatum Offers from Proposers**. Participants played between two blocks (Experiment 2 and Experiment 4: one social and one non-social condition block) and four blocks (Experiment 3 and

Experiment 5: two social and two non-social condition blocks) of the Ultimatum Game as proposers (**Fig S2B**). In each block, participants played (Experiment 2, 3, 5: 72 trails; Experiment 4: 36 trials) against the three different responder groups that differed in their acceptance function (Experiment 2, 3, 5: 24 trials per responder group; Experiment 4: 12 trials per responder group). Each responder group was marked with a neutral shape such as a circle or square and all shapes were randomized for each participant and only used once such that each block consisted of completely novel shapes.

Participants were instructed that they were playing against groups of responders who had received different starting endowments, although they were not told what the endowments were. Hence, participants could anticipate that members from different groups had different expectations but not their direction or form (similar to meeting strangers from different groups for which actors can assume that they may differ in their expectations or implicit norms).

Importantly, while in the social condition, participants were told that they were playing against groups of human responders who had received different starting endowments, in the non-social condition, participants were told that they were playing against computer generated lotteries programmed to mimic the behavior of participants who had received different starting endowments. In other words, they were told that they were playing against computers programmed to behave like humans. One trial from each block was selected at random for payment.

**I.4 Posterior Belief Task**. After one human and one computer block (for Experiments 3-5), participants completed a fully incentivized belief estimation task (**Fig S2C**). In this task, participants were asked to estimate the probability each offer had of being accepted by each responder group against whom they had just played. On each trial, participants were presented with a shape corresponding to one of the responder groups from the previous blocks as well as an offer between 0 and 20. They were asked to identify, on a scale from 0% to 100%, how likely the given offer was to be accepted by a member of that particular responder group. All trials were self-paced. We used a Matching Probability/ auction mechanism to incentivize accuracy (5, 6), and selected one trial at random for payment.

Specifically, participants were instructed that it was in their best interest to estimate the probability of acceptance that was closest to the actual responder's true probability, since this would give them the highest chance of receiving extra payment. The full mechanism of how payoff was determined was as follows: For a given random trial, a participant's estimate of the acceptance probability was compared to a randomly drawn amount between 0 and 100 (the same range available to participants). If the participant's estimate was above the randomly drawn amount, then they would receive a reward with a probability equal to the

true acceptance probability. If the participant's estimate was below the randomly drawn amount, they would receive a reward with a probability equal to the randomly drawn amount. This mechanism guarantees that participants maximize their earnings by reporting their most precise and truthful probability estimation (6, 7), and has been successfully employed in the past (5).

**I.5 Handling of Outliers**. Our pre-registration (https://osf.io/vcweq; https://osf.io/wreaq; https://osf.io/qv5g9; https://osf.io/3fwnt) defined outliers as participants whose data was more than 3 standard deviations above or below the mean for their particular dataset. More specifically, we defined outliers in the learning task as participants whose final offers against any of the three responder groups was more than 3 standard deviations above or below the mean. In the probability matching task, we defined outliers as subjects whose intercepts (of the fitted sigmoid indicating their estimate of the responder group's acceptance function) against any of the responder groups was more than 3 standard deviations above or below the mean. This procedure yielded a total of 10 outliers in the learning task (Experiment 2=0; Experiment 3=5; Experiment 4=5; Experiment 5=0; final *N*=420), and 12 outliers in the probability matching task (Experiment 2=0; Experiment 3=4; Experiment 4=4; Experiment 5=4), with an additional 4 subjects from Experiment 3 being excluded due to incomplete data from technical failure during the probability matching task (final *N*=364). These participants were excluded from further analyses.

**I.6 Supplementary Analysis and Results for Learning.** In order to establish factors that predicted proposer behavior, we performed multilevel regressions using the lme4 package (8) in R (9) and applied Satterthwaite's degrees of freedom method to derive p-values. The regression models included offer made (either limited to trial 1, the final trial, or all offers) as the dependent variable and social (non-social coded as -1, social coded as 1) and responder group (coded numerically as -1, 0, and 1) as independent variables, with the intercept of the model allowed to vary randomly between participants, and participants nested within the experimental sample. The regression equation took the following form:

$$y_{ijk} = \beta_{0jk} + \beta_1 X_{1ijk} + e_{ijk},\ e_{ijk} \sim N(0, \sigma_e^2) \quad \text{(level-1)}$$
$$\beta_{0jk} = \beta_{0k} + e_{0jk},\ e_{0jk} \sim N\left(0, \sigma_{e_{0jk}}^2\right) \quad \text{(level-2)}$$
$$\beta_{0k} = \beta_0 + e_{0k},\ e_{0k} \sim N\left(0, \sigma_{e_{0k}}^2\right) \quad \text{(level-3)}$$

where $k$ = experimental sample, $j$ = subject, $i$ = offer

The same procedure was repeated for payoff. When analyzing experiments separately, we obtained the same direction and significance for all parameters, and hence collapsed across experiments in the final analysis (see **Table S1**). However, below we also provide forest plots showing the effects of each experiment separately for each variable of interest (see **Fig S3**).

**Table S1**: Multi-level regression on offers and payoff

| | Initial Offer<br>B (se) | Avg. Offer<br>B (se) | Final Offer<br>B (se) | Payoff<br>B (se) |
|---|---|---|---|---|
| Intercept | 8.013 (0.135) *** | 7.132 (0.218) *** | 7.038 (0.212) *** | 10.469 (0.079) *** |
| Non-social vs. Social | 0.416 (0.040) *** | 0.212 (0.009) *** | 0.173 (0.039) *** | -0.055 (0.019) ** |
| Resp. Group | 0.068 (0.049) | -0.937 (0.011) *** | -1.343 (0.047) *** | 2.910 (0.024) *** |
| NS/S × Resp. Group | 0.036 (0.049) | 0.088 (0.011) *** | 0.103 (0.047) * | -0.178 (0.024) *** |
| Observations | 420 | 420 | 420 | 420 |

*Note*. *** $p < 0.001$, ** $p < 0.01$, * $p < 0.05$, # $p < 0.10$ (two-tailed tests). Analyses based on pooled data of four experiments (see *Methods*, main Text).

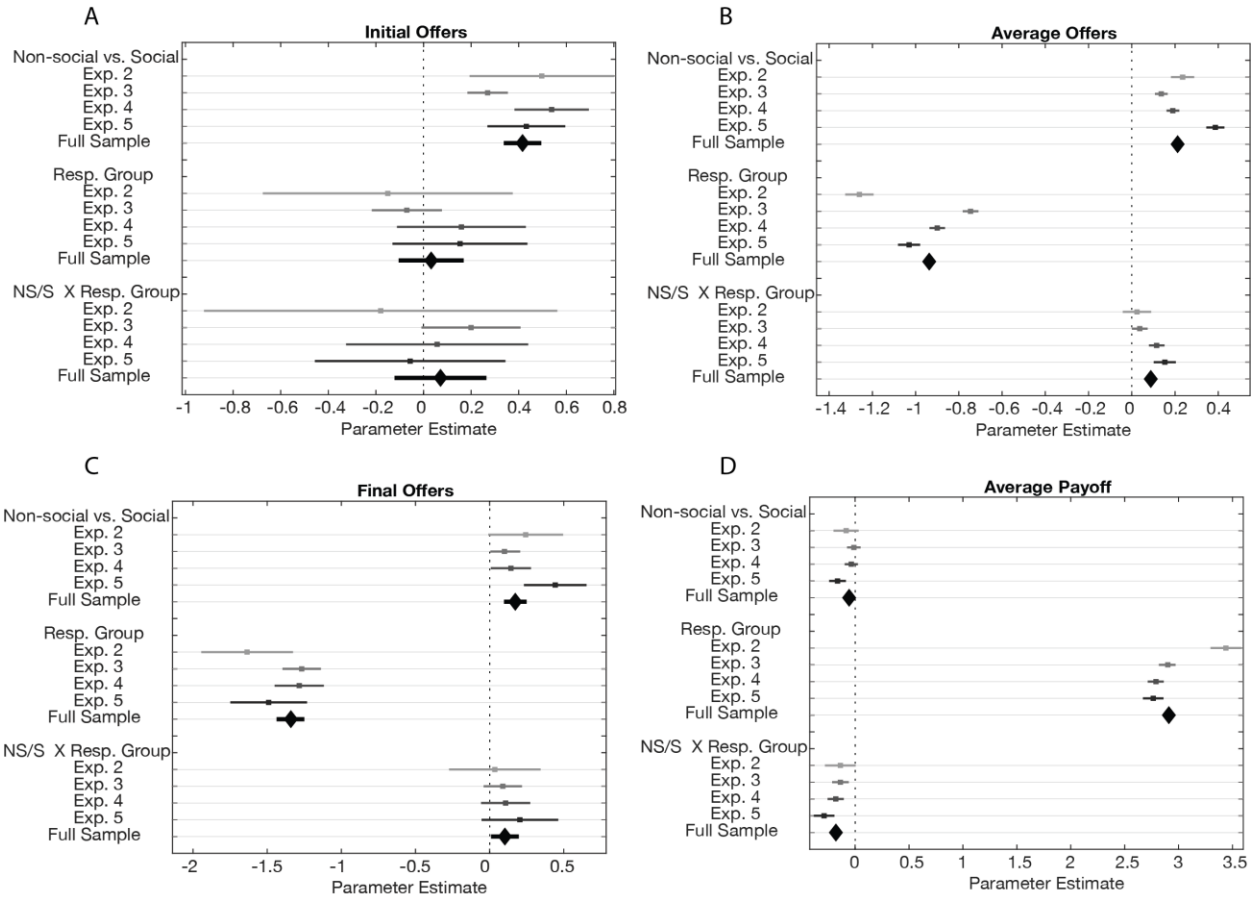


**Figure S3. Behavioral results per experiment.** Initial offer (**A**), average offer (**B**), final offer (**C**), and average payoff (**D**). Each square represents the regression coefficient in one of our experiments, diamonds represent effects from all experiments pooled together, error bars represent 95% confidence intervals. Error bars that no not cross the vertical dotted line indicate a significant effect at $p < 0.05$.

To exclude the possibility that any results could be caused by an alteration of behavioral strategies following the elicitation of beliefs, we re-ran the above analyses excluding all blocks of trials that followed our belief estimation task. This resulted in half of all trials being eliminated for Experiments 3-5 (Experiment 2 did not include the belief elicitation task). The pattern of results presented above remained when excluding these trials.

**I.7 Risk-aversion in Ultimatum Bargaining.** An alternative to inequality aversion may be risk aversion. This would assume that individuals with strong risk aversion make more generous opening offers and that this is especially the case when interacting with human (compared to computer) responders. If true, risk rather than inequality aversion may explain the differential learning of responder group acceptance thresholds. To examine this alternative possibility, participants in both Exp. 2 and 5 were, at the end of the entire experimental session, asked to complete the Eckel-Grossman Risk Task (10). In this task, participants are presented with six gambles, each of which results in either a high or a low payout with equal probability (i.e., 50%). The six gambles differ in their high and low payouts, thereby systematically varying the level of risk between gambles. For example, the safest gamble has a high and low payout of 28MU, while the riskiest gamble has a high payout of 70MU and a low payout of 2MU. Participants are asked to select only one gamble, and this selection is used as a measure of their risk preference.

We computed regression models with Initial Offer as the criterion, and the social/non-social treatment, risk-preference, and their interaction as predictors. For experiment 2, we found the main effect for treatment ($p$ = 0.05), no effect for risk-preference ($p$ = 0.93), and no interaction effect ($p$ = 0.59). For the fMRI experiment 5, we likewise found the main effect for treatment ($p$ = 0.009), no effect for risk-preference ($p$ = 0.96), and no interaction effect ($p$ = 0.75). From these results, we infer that risk-preferences neither systematically predict initial offers nor provide evidence that risk preferences influence initial offers of participants. Importantly, differences in risk preferences also fail to explain the different offer-rates we observe across the social/non-social treatment. As such, risk preferences do not provide an alternative mechanism for the treatment effect in our datasets.

**I.8 Supplementary Analysis and Results – Probability Matching Task**. To test for differences in posterior beliefs, we first submitted our participants' raw estimates of each offer's acceptance probability to multilevel regressions. The regression models included the estimated probability that an offer would be accepted as the dependent variable and offer (0 through 20), social (non-social coded as -1, social coded as 1) and responder group (coded numerically as -1, 0, and 1) as well as the interaction between social and responder group as independent variables, with the intercept of the model allowed to vary randomly between participants, and participants nested within experimental sample. **Table S2** presents results from

this analysis from all experiments.

As an alternative to the above (model-free) regressions, we further employed a model-based approach. We used MATLAB's (Mathworks) glmfit function in order to fit sigmoid functions to each subject's raw estimate of acceptance likelihood for each offer (see Main Text, **Fig 4B**). This procedure resulted in, for each subject, a slope and intercept value for each responder group in both the social and non-social conditions. These intercepts provide an indication of each subject's estimate of each responder group's acceptance function. We then submitted these intercepts to paired *t*-tests in order to probe for differences between social and non-social beliefs. Based on the model simulations, we expected most pronounced differences in the most lenient responder culture (responder endowment = 20). **Table S3** shows the results.

**Table S2**: Multi-level regression on estimates of offer acceptance

| | B (se) |
|---|---|
| Intercept | 6.400 (3.811) |
| Offer | 5.794 (0.022) *** |
| Non-social vs. Social | -0.154 (0.108) |
| Resp. Group | 5.114 (0.132) *** |
| NS/S × Resp. Group | -0.319 (0.132) * |
| Observations | 364 |

*Note*. *** $p < 0.001$, ** $p < 0.01$, * $p < 0.05$, # $p < 0.10$ (two-tailed tests). Analyses based on pooled data of three experiments (see *Methods*, main Text).

**Table S3**: *t*-tests on intercepts from model-based analysis

| | *Social mean (se)* | *Non-social mean (se)* | *t*-stat |
|---|---|---|---|
| Resp. Group A | -4.050 (0.154) | -3.953 (0.155) | -0.771 |
| Resp. Group B | -3.361 (0.109) | -3.493 (0.178) | 0.991 |
| Resp. Group C | -3.038 (0.141) | -2.741 (0.145) | -2.290 * |
| Observations | 364 | 364 | 364 |

*Note*. All contrasts are between non-social and social conditions. *** $p < 0.001$, ** $p < 0.01$, * $p < 0.05$, # $p < 0.10$ (two-tailed tests). Analyses based on data of three experiments (see *Methods*, main Text).

**Table S4**: *t*-tests on slopes from model-based analysis

| | *Social mean (se)* | *Non-social mean (se)* | *t*-stat |
|---|---|---|---|
| Resp. Group A | 0.564 (0.023) | 0.538 (0.020) | 1.524 |
| Resp. Group B | 0.572 (0.023) | 0.581 (0.028) | -0.451 |
| Resp. Group C | 0.609 (0.034) | 0.595 (0.034) | 0.481 |
| Observations | 364 | 364 | 364 |

*Note*. All contrasts are between non-social and social conditions. *** $p < 0.001$, ** $p < 0.01$, * $p < 0.05$, # $p < 0.10$ (two-tailed tests). Analyses based on data of three experiments (see *Methods*, main Text).

**Table S5**: *t*-tests on estimates of offer acceptance for all offers

| Offer | Resp. Group A | | Resp. Group B | | Resp. Group C | | Observations |
|---|---|---|---|---|---|---|---|
| | *t*-stats | | *t*-stats | | *t*-stats | | |
| | behavior | model | behavior | model | behavior | model | |
| 0 | -1.837 # | 0.42 | -2.655 ** | -1.578 | -2.838 ** | -2.866 ** | 364 |
| 1 | -1.002 | 0.512 | -1.249 | -1.256 | -3.241 ** | -2.686 ** | 364 |
| 2 | -0.775 | 0.496 | -1.116 | -0.814 | -2.311 * | -2.371 * | 364 |
| 3 | 0.123 | 0.402 | 0.038 | -0.29 | -1.828 # | -2.106 * | 364 |
| 4 | 0.874 | 0.337 | 0.706 | 0.166 | -1.2 | -1.785 # | 364 |
| 5 | 1.602 | 0.368 | 1.2 | 0.388 | -1.026 | -1.313 | 364 |
| 6 | 0.927 | 0.422 | 0.339 | 0.358 | 0.129 | -0.889 | 364 |
| 7 | -0.004 | 0.409 | 0.68 | 0.297 | -1.14 | -0.533 | 364 |
| 8 | -0.436 | 0.46 | -1.33 | 0.284 | 0.242 | -0.26 | 364 |
| 9 | -0.382 | 0.527 | -0.686 | 0.23 | -0.619 | -0.183 | 364 |
| 10 | 0.996 | 0.461 | 0.088 | 0.102 | -0.351 | -0.252 | 364 |
| 11 | -0.376 | 0.316 | -0.343 | -0.045 | 0.909 | -0.367 | 364 |
| 12 | 1.225 | 0.138 | 0.765 | -0.188 | -0.054 | -0.481 | 364 |
| 13 | 1.204 | -0.037 | 0.484 | -0.325 | 0.955 | -0.572 | 364 |
| 14 | 0.601 | -0.164 | 1.38 | -0.459 | 0.925 | -0.626 | 364 |
| 15 | 0.907 | -0.229 | 1.019 | -0.585 | 0.754 | -0.642 | 364 |
| 16 | 1.634 | -0.72 | 0.6 | 0.986 | 2.404 * | -0.621 | 45 |
| 17 | 0.621 | -0.69 | 0.969 | 0.88 | -0.894 | -0.564 | 45 |
| 18 | 1.702 # | -0.677 | 0.87 | 0.762 | 0.998 | -0.507 | 45 |
| 19 | -0.281 | -0.679 | -1.195 | 0.637 | -0.502 | -0.449 | 45 |
| 20 | -0.754 | -0.694 | 1.508 | 0.509 | -0.097 | -0.39 | 45 |

*Note*. All contrasts are between non-social and social conditions. *** $p < 0.001$, ** $p < 0.01$, * $p < 0.05$, # $p < 0.10$ (two-tailed tests). Analyses based on data of three experiments (see *Methods*, main Text).

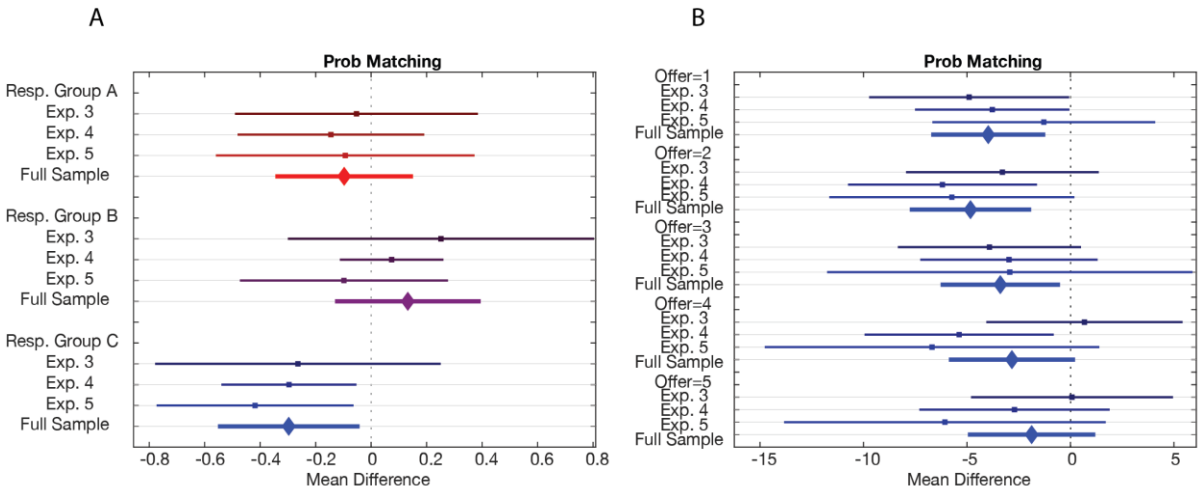


**Figure S4. Probability matching results for all experiments.** Shown are the results for analyses on the intercept (A) as well as the average offer for responder group C (B), separated by experiment. Each square represents the mean difference in one individual experiment, diamonds represent effects from all experiments pooled together, error bars represent 95% confidence intervals. Error bars that do not cross the vertical dotted line indicate a significant effect at $p < 0.05$.

## II. Computational Model and Simulations

**II.1 Model Fitting and Parameter Optimization.** The classic Maximum Likelihood (ML) approach estimates model parameters $\theta_M$ by finding the values which minimize the negative logarithm of the likelihood (nLL) of observed choices D given the model M and parameter values $nLL = -\log(P(D \mid M,\theta_M))$. Alternatively, model parameters $\theta_M$ can be estimated by finding the values which minimize the negative logarithm of the posterior probability (nLPP). This term is computed as $nLPP = -\log(P(\theta_M \mid D,M)) \propto -\log(P(D \mid M,\theta_M)) - \log(P(\theta_M \mid M))]$, where $P(D \mid M,\theta_M)$ is the likelihood of the data (i.e., the observed offer) given the considered model M and parameter values $\theta_M$, and $P(\theta_M \mid M)$ is the prior probability of the parameters. This Maximum A Posterior (MAP) approach can be used to regularise parameters. It avoids that some parameters take extreme values or constrain parameters to some theoretical bounds, by choosing appropriate prior distributions for the parameters $P(\theta_M \mid M)$ – see also (11). Here we used a MAP approach with an L-BFGS-B algorithm (12) for optimization of the parameter search, as implemented in Matlab's fmincon function, initialized at multiple, random starting points of the parameter space (10 iterations).

Following modelling state-of the art practices (13), we performed a parameter recovery analysis to verify that it was possible to estimate the model parameters (see section **II.2**). We also compared the parameters obtained with the nLL and MAP approaches to assess if and how the chosen prior distributions biased the parameter estimation (see section **II.3**).

**II.2 Model Identifiability & Parameter Recovery**. Following standard practices in the field of computational modelling, we performed both model identification and parameter recovery analyses (13).

For the parameter recovery analysis, we focused on our candidate model, which includes the inequality aversion in the social condition and, hence, has 6 parameters ($\beta$, $\mu_1$, $\mu_2$, $\Sigma_1$, $\Sigma_2$, $\omega$). We ran 10 simulations, each containing 50 synthetic subjects. Task properties and contingencies used for the simulations were following and, therefore, identical to the fMRI study design (288 trials: 2 social conditions × 3 cultures × 24 trials × 2 repetitions). We used randomly sampled learning model parameters from the same prior distributions used to calculate LPP in model fitting, which roughly approximate the distribution of parameters estimated from actually fitting the model to our actual participants (see Main Text). We then assessed the parameter recovery in two ways: first, we ran a robust regression between the input parameters and the estimated parameters for all synthetic subjects (500 = 10 × 50). We then used the estimated regression parameters (intercept $B_0$ and slope $B_1$) to assess how well our parameter estimation procedure can actually retrieve specific parameter values (**Fig S5A**). In the case of perfect estimation, those regressions should feature intercepts close to 0 and slopes close to 1 ($B_0 = 0$ and $B_1 = 1$), with a maximally explained variance ($R^2 \sim 1$).

Next, we computed the Pearson correlation between the parameters used to generate the data and the parameters estimated in each simulation. We then averaged the R and $R^2$ over the 10 simulations and plotted those as confusion matrices (**Fig S5B**) to assess how well our parameter estimation procedure captures the inter-individual differences in a typical n = 50 experiment (on-diagonal terms), and how much multicollinearity between the different parameters is produced by the estimation procedure (off diagonal terms). In the case of perfect parameter estimation, these confusion matrices should feature diagonal terms close to 1 and off-diagonal terms close to 0. Overall, our results suggest that our model parameters are satisfactorily estimated by our fitting procedure (**Fig S5**).

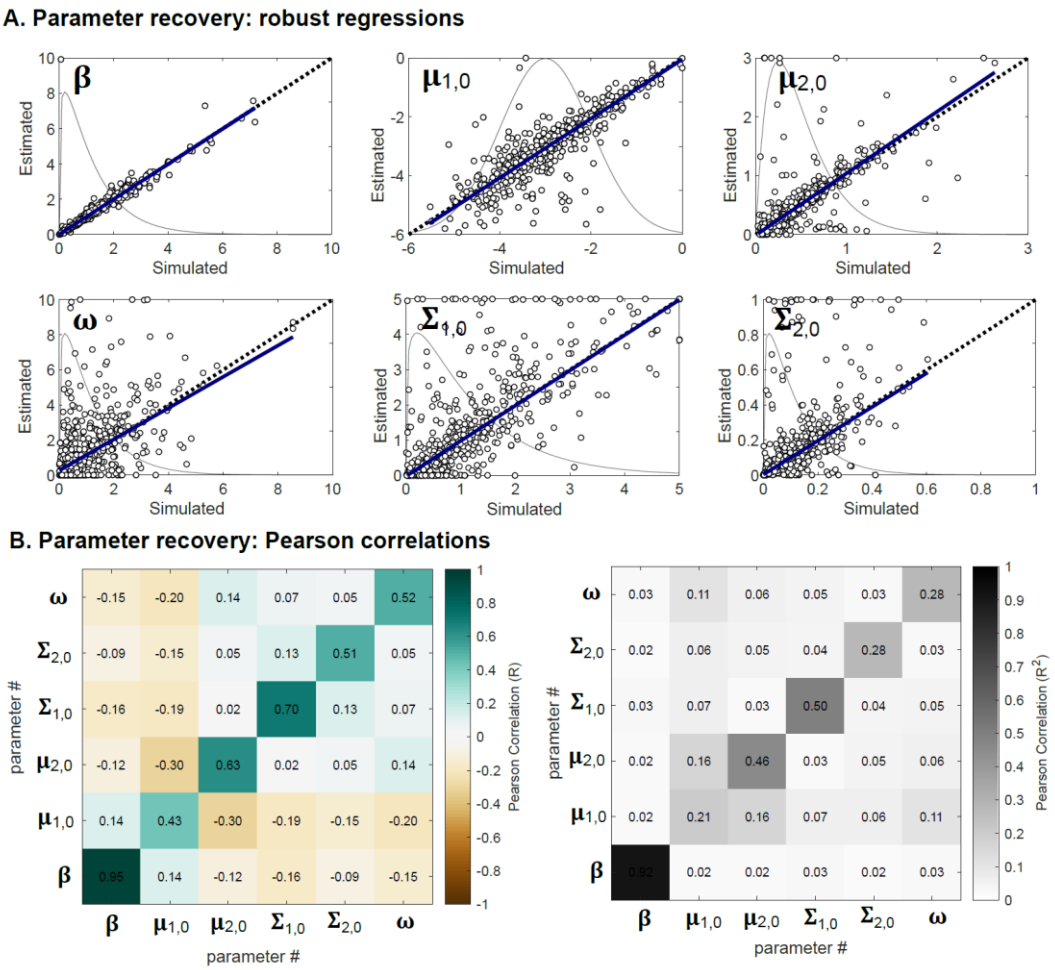


**Figure S5. Parameter recovery analysis. A.** Robust regressions. Data from 500 synthetic participants (10 simulations × 50 individuals) were simulated with the alternative model (with IA). The 6 estimated parameters per participants were then regressed against the true parameters used for simulating the data, using robust regressions. Results show very good identifiability, with robust regression intercepts close to 0, robust regression slopes close to 1 and high statistical significance (all *p*-values close to Matlab's precision – i.e. reported as 0). Each dot represents a synthetic individual. The black dotted lines represent the identity line and the thick, blue, continuous lines the best linear fits (robust regression). The grey densities represent the probability distributions used to sample the parameters. **B.** Pearson correlations. The confusion matrices represent summary statistics of the correlations between parameters, estimated over 50-subjects simulations, and averaged over the 10 simulations. Diagonal: correlations between simulated and estimated parameters. Off diagonal: cross correlation between estimated parameters. Left: Pearson correlation (R). Right: explained variance ($R^2$).

For the model identification analysis, we focused on the comparison between our candidate model and a null model that does not includes the inequality aversion in the social condition, hence only possesses 5 parameters ($\beta$, $\mu_1$, $\mu_2$, $\Sigma_1$, $\Sigma_2$, $\omega$). We ran 10 simulations, each containing 50 synthetic subjects, with each of those two models, randomly sampling learning model parameters from our prior distributions. Then, for each of the two generating model scenarios, we fitted both models of the model space, computed the model comparison metric (the Laplace Approximation to Model Evidence) with the estimated parameters, and ran

a Bayesian model comparison between those 2 models. We then computed the conditional probability that a model fits best given the true generative model p(est.|sim.), and the conditional probability that the data was generated by a specific model, given that the model was observed as providing the best fit to the generated data p(sim.|est.). In the case of perfect identification, these confusion matrices should feature diagonal terms close to 1 and off-diagonal terms close to 0. Overall, our results show a good identification of our models (**Fig S6**).

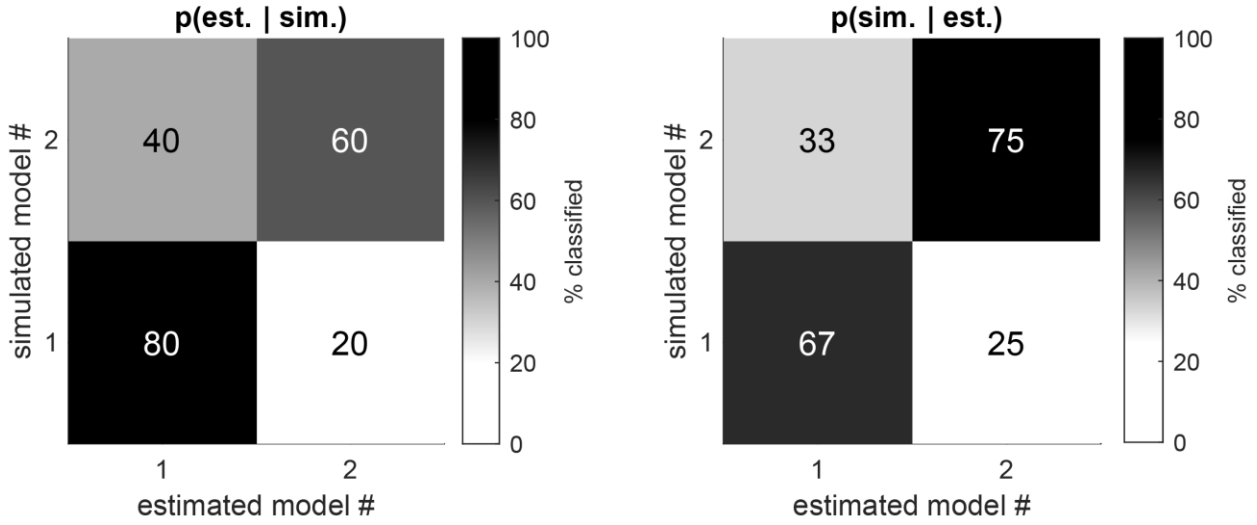


**Figure S6. Model identifiability analysis.** Data from 50 synthetic participants were simulated with each of our two models (null model (#1) and alternative model (#2)). Bayesian model selection was used to identify the most probable model generating the data, using model exceedance probability. This procedure was repeated 10 times. We then computed the conditional probability that a model fits best given the true generative model p(est.|sim.) (left), and the conditional probability that the data was generated by a specific model, given that the model was observed as providing the best fit to the generated data p(sim.|est.) (right).

**II.3 Parameter Estimates**. In this section, we provide a full description of the model parameters distributions estimated from our data (**Fig S7**). Although the use of priors or other hierarchical estimation procedure is often portrayed as a good practice and an efficient way to regularize parameters (11), there is often little appreciation of how much the use of those techniques impact the estimation of parameters. Here we provide such an estimation, by comparing the distribution of parameters obtained using a simple maximum Likelihood (nLL) estimation procedure and the value of parameters obtained using a maximum A Posteriori (MAP) estimation procedure with our chosen prior distributions which were as follows: inverse temperature parameter ($\beta$) was sampled in a Gamma distribution defined by a shape $a$ and scale $b$ parameter ($a$ = 1.2, $b$ = 1). Intercept of the belief function ($\mu_1$) was sampled in a Normal distribution defined by mean ($\mu$) and standard deviation ($\sigma$) ($\mu$ = -3, $\sigma$ = 1). The slope of the belief function ($\mu_2$) was sampled in a Gamma distribution defined by a shape $a$ and scale $b$ ($a$ = 2, $b$ = 0.25). The variance around the intercept of the

belief function ($\Sigma_1$) was sampled in a Gamma distribution defined by a shape *a* and scale *b* (*a* = 1.2, *b* = 1). The variance around the slope of the belief function ($\Sigma_2$) was sampled in a Gamma distribution defined by a shape *a* and scale *b* (*a* = 1.2, *b* = 0.1). Finally, the weight of inequality aversion (ω) was sampled in a Gamma distribution defined by a shape *a* and scale *b* (*a* = 1.2, *b* = 0.1). Our result show that, at the population level, the inclusion of the prior in the MAP procedure does not appear to distort the estimation, compared to the nLL procedure (**Fig S7**).

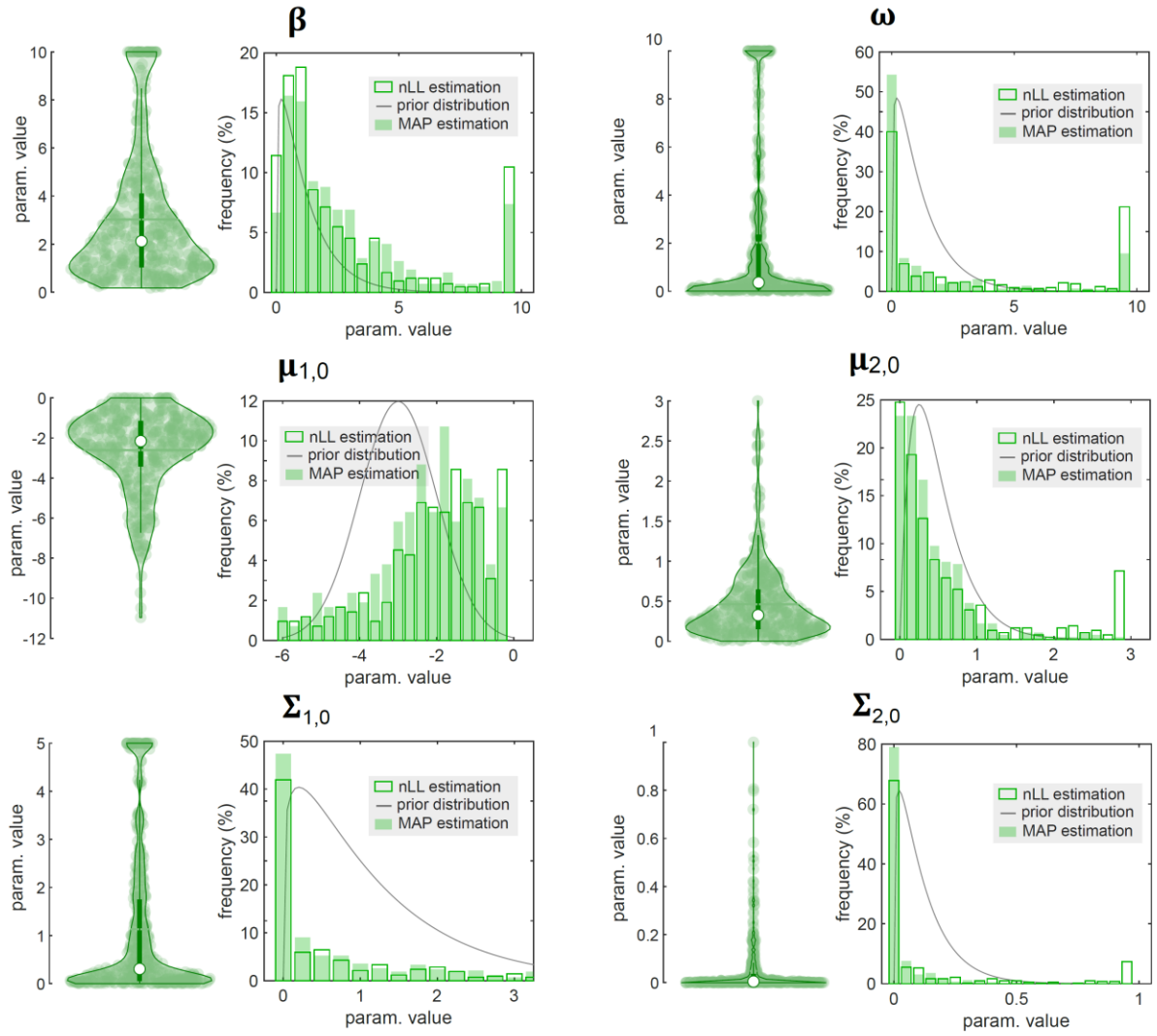


**Figure S7. Parameter distributions.** For each of our six model parameters, the left panel is a violin plot of the parameters estimated with the MAP procedure in our full sample (n = 420). In the violin plots panels, the white dots represent the sample median, the horizontal green bar the sample mean, the thick central line indicates the 25-75% quantiles, and the thin central line indicates the 5-95% quantiles. The light-colored dots represent all individual datapoints. For each of our six model parameters, the right panel is a histogram depicting the distribution of the

parameters estimated with the MPA (green-fill histogram) and the nLL procedure (green-edge histogram). The light grey curve indicates the prior distribution used in the MAP procedure.

**II.4 Learning Model – Simulations & Falsification**. In this section, we detail the result of simulations obtained with our null and our alternative model – a procedure also known as *model falsification* (14). The idea is to show that our alternative model reproduces specific qualitative patterns of behavior that the null model does not. To do so, we first fitted the two models with the MAP procedure. We then simulated 420 synthetic individuals with each model, using the vector of estimated parameters from each of the 420 participants in our full sample. We then submitted the simulated behavior to the same analyses as the participants behavior, to assess which model better captures the key behavioral patterns observed in our task and conditions/treatments. This means the same hierarchical regressions were estimated. The full results of this are provided in **Table S6**, with results from behavioral data likewise included to help facilitate comparison between behavioral and model-simulated results.

**Table S6**: Multi-level regression on offers and payoff

| | Initial Offer<br>B (se) | Avg. Offer<br>B (se) | Final Offer<br>B (se) | Payoff<br>B (se) |
|---|---|---|---|---|
| Non-social vs. Social | | | | |
| Data | 0.416 (0.040) *** | 0.212 (0.009) *** | 0.173 (0.039) *** | -0.055 (0.019) ** |
| Null model | -0.008 (0.050) | -0.009 (0.009) | -0.010 (0.038) | 0.008 (0.010) |
| Alternative model | 0.163 (0.046) *** | 0.190 (0.009) *** | 0.118 (0.038) ** | -0.067 (0.010) *** |
| Resp. Group | | | | |
| Data | 0.068 (0.049) | -0.937 (0.011) *** | -1.343 (0.047) *** | 2.910 (0.024) *** |
| Null model | -0.016 (0.061) | -1.023 (0.011) *** | -1.526 (0.046) *** | 1.871 (0.012) *** |
| Alternative model | -0.040 (0.057) | -1.009 (0.011) *** | -1.522 (0.047) *** | 1.790 (0.012) *** |
| NS/S × Resp. Group | | | | |
| Data | 0.036 (0.049) | 0.088 (0.011) *** | 0.103 (0.047) * | -0.178 (0.024) *** |
| Null model | -0.059 (0.061) | -0.006 (0.011) | 0.028 (0.046) | 0.020 (0.012) |
| Alternative model | 0.006 (0.057) | 0.071 (0.011) *** | 0.093 (0.047) * | -0.131 (0.012) *** |
| Observations | 420 | 420 | 420 | 420 |

*Note*. *** $p < 0.001$, ** $p < 0.01$, * $p < 0.05$, # $p < 0.10$ (two-tailed tests). Analyses based on pooled data of four experiments (see *Methods*, Main Text).

**II. 5 Individual Time-series**. In this section, we provide a more detailed overview of our computational model, as well as its ability to capture different individual patterns of behavior. To do so, we focused on individual behavioral time series and created a graphical representation that allows a visual comparison of how well model predictions (i.e., likelihood of potential offers) match actual behavior (i.e., actual offers made), as well as how the succession of accept/reject experiences shape the trajectories of those variables in all conditions. We selected two participants from the fMRI sample, who exhibited prototypical behavior.

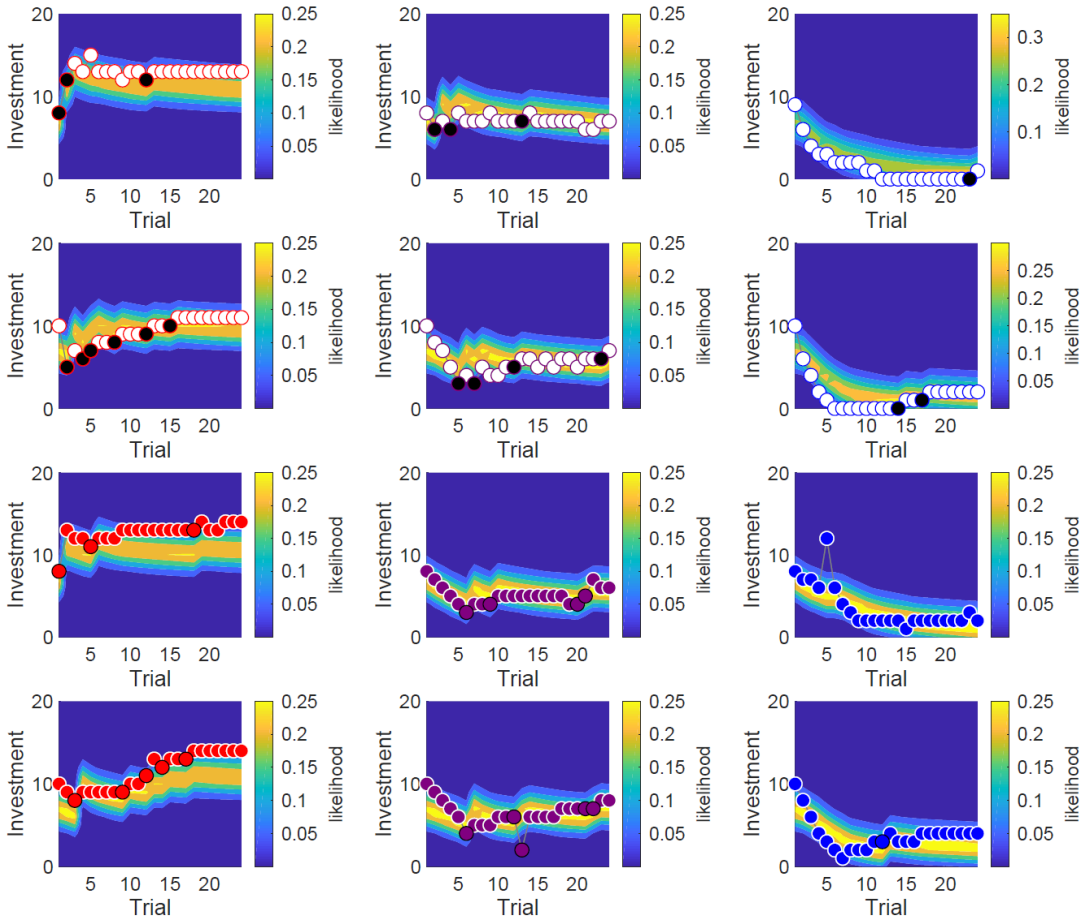


**Figure S8. Individual time series and model prediction (1).** Each panel represents the time series and model predictions of one fMRI cohort individual's behavior (i.e., investment as a function of trial number) for one specific condition (i.e., opponent group A: red, B: purple; C: blue) in the social (color-filled symbols) or non-social (white-filled symbols) treatment. Because the design featured two repetitions, this led to 12 panels (3 opponents × 2 treatments × 2 repetitions), the upper line of each condition consisting of the first repetition and the lower line the second repetition. In each panel, the dot symbols represent the actual behavior (i.e., observed investment), at each trial. Colored and white symbols indicate that the offer was accepted by the opponent, and black symbols that the offer was rejected by the opponent. One can see that investments tend to decrease after accepted offers, and increase after rejected offers. The color-scaled background indexes the likelihood of observing each potential investment at each trial, as computed by our alternative model, after fitting the individual parameters to each subject's behavior (see *Methods*, Main Text). Yellow-color indicate high likelihood, and blue low likelihood. One can observe that the likelihood surface is yellow in the vicinity of the observed behavior and blue elsewhere, indicating that the model nicely captures the dynamic of the behavior of this specific subject. The chosen subject here features a fairly

prototypical behavior, with a characteristic learning pattern (offers increase against opponent A and decrease against opponent C) and inequality aversion (offers are higher in the social than in the non-social condition). It is notable that against the most lenient opponent (C: blue), the offers at the end of learning are still significantly higher in the social than in the non-social condition.

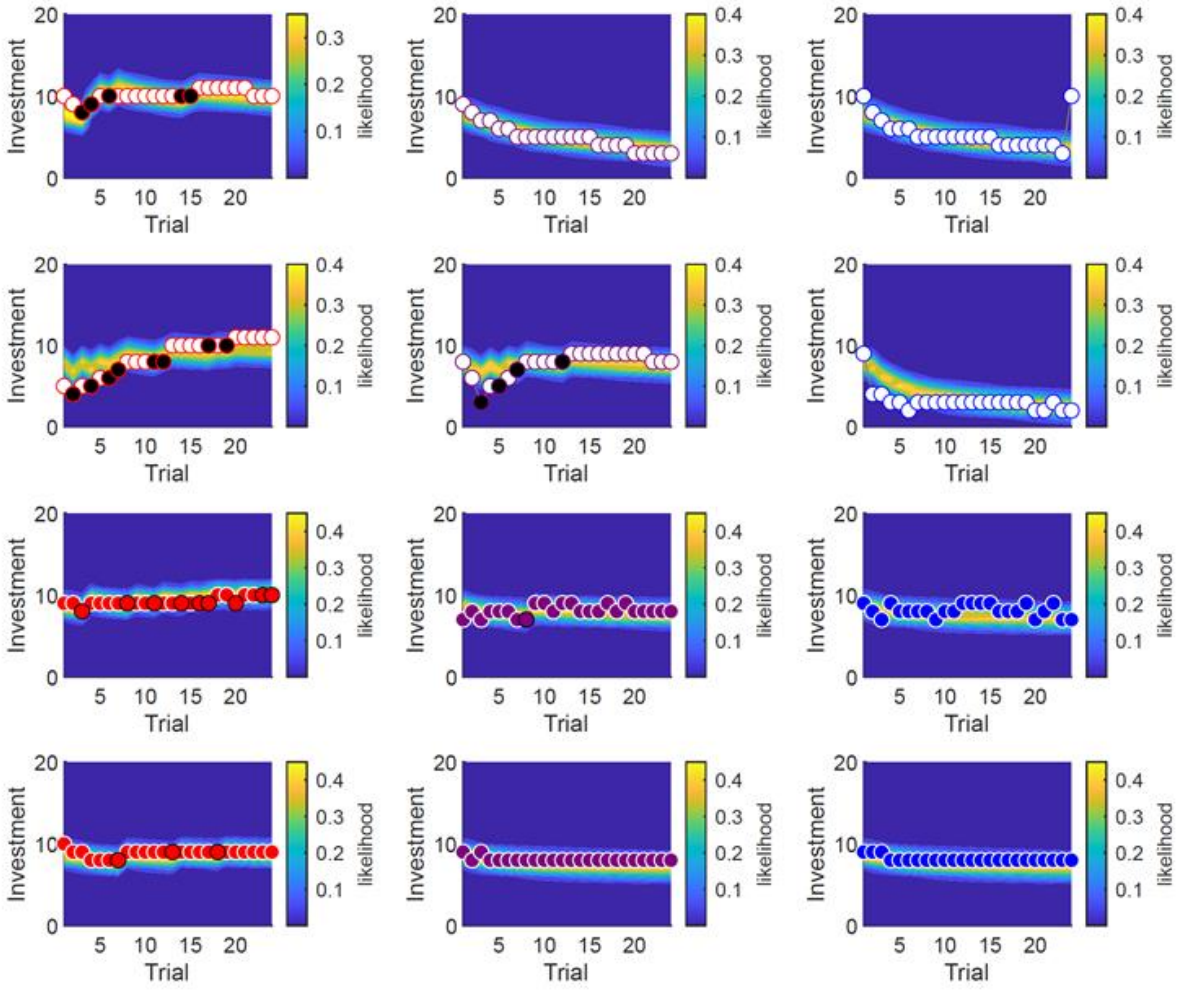


**Figure S9. Individual time series and model prediction (2).** For a detailed caption, see **Fig S8**. The chosen subject here exhibits a different strategy: a characteristic learning pattern in the non-social condition only (offers increase against opponent A, and decrease against opponent C). The behavior in the social condition is dominated by inequality aversion: there is no learning, and all offers are close to a fair split of the endowment (10). Despite the strategy of this individual being very different from **Fig S8**, our model was able to adjust to the data to fully capture this alternative pattern of behavior.

**II.6 Efficiency.** To formalize the intuition that inequality aversion leads agents to become overly generous and to make inefficient (i.e., uninformative) offers when interaction partners have (unobservable) low acceptance thresholds and would accept more self-serving actions, we adopted the A-optimality criterion from optimal design theory. A-optimality criterion can indeed be used to assess the efficiency of an option O to estimate the receiver's parameters. Formally, an A-optimal offer minimizes the trace of the inverse of

the Fisher information matrix – which corresponds to the reciprocal of the variance of the estimator. In other words, efficient offers use current beliefs to evaluate which offer would generate feedback that would be most informative to get accurate estimates of posterior beliefs. Thereby, we computed our measure of offer-efficiency as the negative trace of the posterior variance-covariance matrix on parameters of the acceptance function $-tr(\Sigma_{t+1})$. Applied to the simulations reported in the main text (**Main Figure 1-2**), these new analyses show that the presence of inequality aversion in the social condition indeed leads agents to make more inefficient (i.e., uninformative) offers (**Figure S10 AB**). This pattern develops over time and particularly worsen in the most lenient responder group (**Figure S10 C**).

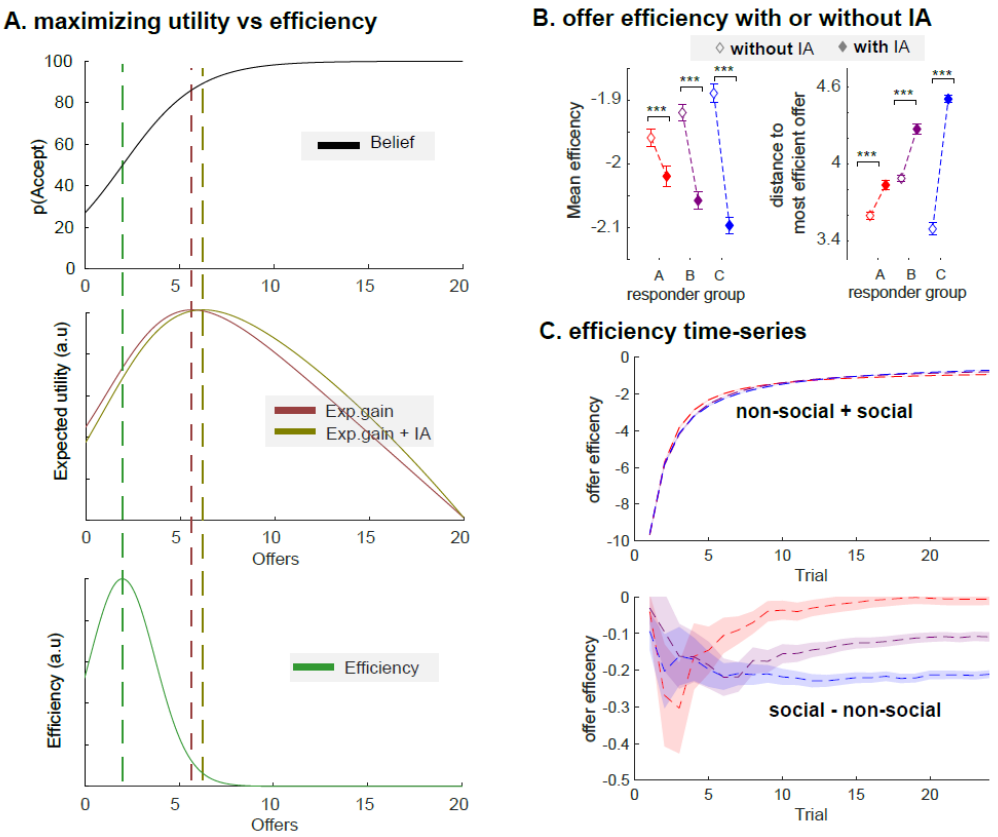


**Figure S10. offer efficiency. A.** Optimal offer for Utility vs Efficiency. Top panel: at a certain trial, an agent holds a certain belief about the acceptance function of the responder group. Middle panel: This function can be used to derive the offer that maximizes the agent's expected gain (non-social condition, red), or its expected utility − i.e., expected gain + inequality aversion− (social condition, brown-green). Bottom panel: given the agent's current belief, one can also compute the efficiency of different offers (green). In this case, the offer that maximizes the expected utility is far less efficient than the most efficient offer and also less efficient than the offer that maximizes the expected gain. Colored, vertical dashed lines indicate offers that maximize the respective colored functions (red: expected gain; brown-green: expected utility; green: efficiency) **B.** We computed the efficiency of the offers made in the simulated behavior (Main Figure 2). Left panel: Results show that the offer mean efficiency is higher without the inequality aversion term (i.e., in non-social context) than with the inequality aversion term (i.e., in the social context). Right panel: consequently, the distance to the most efficient offer is higher with the inequality aversion term (i.e., in the social context) than without the inequality aversion term (i.e., in non-social context). In both cases, the inefficiency is highest in the most lenient responder group (blue). **C.** Time series of offer efficiency. The time-course depicts the evolution of the offer efficiency generated from the simulated behavior (Main Figure 2) in all conditions (both non-

social and social, top) and as a function of the social condition (social – non-social; right), for the three different responder groups, depicted with different colors (red = responder group A; purple = responder group B; blue = responder group C). Whereas the top graph illustrates that learning generally improves the efficiency of offer made over time, the bottom graph specifically shows the effect of the inequality aversion term (present in the social, and not in the non-social condition), on the efficiency of the offers made to the different responder groups.

**II.7 Gaussian-Newton Algorithm**. The variational-Laplace scheme was implemented using the routines of the VBA toolbox (15). Note that, under certain circumstances (when the Hessian is badly conditioned), the convergence of the standard Newton optimization algorithm used by default in the VBA toolbox is not guaranteed. We therefore modified the Gauss-Newton optimization algorithm, according to the following reasoning.

Let $f: x \to f(x)$ be a function, whose maximum $x^*$ we want to identify.

First, consider the following 2nd-order Taylor expansion of $f(x)$:

$$f(x) \approx f(x_0) + \underbrace{\left.\frac{\partial f}{\partial x}\right|_{x=x_0}}_{J(x_0)} (x - x_0) + \frac{1}{2}(x - x_0)^T \underbrace{\left.\frac{\partial^2 f}{\partial x^2}\right|_{x=x_0}}_{H(x_0)} (x - x_0) + \ldots \tag{1}$$

where $x_0$ is some initial guess of the unknown maximum $x^*$, $J(x_0)$ is the gradient of $f$ wrt $x$, and $H(x_0)$ is its Hessian.

Now let $\tilde{f}: x \to \tilde{f}(x)$ be defined as:

$$\tilde{f}(x) = f(x_0) + J(x_0)(x - x_0) + \frac{1}{2}(x - x_0)^T H(x_0)(x - x_0) \tag{2}$$

A standard Newton optimization step simply assumes that $\tilde{f}(x)$ is a good approximation of $f(x)$ in the neighborhood of $x_0$, and thus proposes to move from $x_0$ to $\tilde{x}^*$, which is (by definition) the optimizer of $\tilde{f}$.

First, note that the gradient of $\tilde{f}$ is given by:

$$\frac{\partial \tilde{f}}{\partial x} = (x - x_0) + H(x_0)(x - x_0) \tag{3}$$

If $\tilde{x}^*$ is the optimizer of $\tilde{f}$, then by definition:

$$\left.\frac{\partial \tilde{f}}{\partial x}\right|_{x=\tilde{x}^*} = 0 \tag{4}$$

And therefore (setting $x = \tilde{x}^*$ in Equation 3):

$$0 = J(x_0) + H(x_0)(\tilde{x}^* - x_0) \Rightarrow \tilde{x}^* = x_0 - H(x_0)^{-1} J(x_0) \tag{5}$$

This yields the standard Newton optimization algorithm, whose pseudo code is given below:

**Initialize** $x^* = x_0$

**While** [convergence criterion is not met]

Update $x^* \leftarrow x^* - H(x^*)^{-1} J(x^*)$

End

This, however, can diverge when the Hessian is badly conditioned.

The following modified Gauss-Newton algorithm actually performs much better in most circumstances:

**Initialize** $x^* = x_0$

**While** [convergence criterion is not met]

Evaluate cost function before the step: $I^* = f(x^*)$

Derive Gauss-Newton (double) step: $\Delta x = -2 \times H(x^*)^{-1} J(x^*)$

**While** [cost function after the step does not decrease]

Halve step: $\Delta x = \Delta x / 2$

Evaluate cost function after the step: $I = f(x^* + \Delta x)$

End

Update $x^* \leftarrow x^* + \Delta x$

End

Example for a binomial likelihood with gaussian priors.

Let $f(x)$ be the following log posterior probability density:

$$f(x) = \underbrace{y \log s \circ g(x) + (1-y) \log(1 - s \circ g(x))}_{\text{log (bernouilli) likelihood term}} \underbrace{- \frac{1}{2}(x - \mu_0)^T \Sigma_0^{-1} (x - \mu_0)}_{\text{log (Gaussian) prior term}} \tag{6}$$

where $x$ is some hidden cause of the data that controls its first-order moment through some (possibly nonlinear) function $g(x)$ mapped through the standard sigmoid $s : x \to 1/1 + e^{-x}$.

First, note that the function $f(x)$ can be re-written as:

$$
\begin{aligned}
f(x) &= y \log s \circ g(x) + (1-y) \log\left(1 - s \circ g(x)\right) - \frac{1}{2}(x-\mu_0)^T \Sigma_0^{-1}(x-\mu_0) \\
&= y \log s \circ g(x) + (1-y)\left(\log s \circ g(x) - g(x)\right) - \frac{1}{2}(x-\mu_0)^T \Sigma_0^{-1}(x-\mu_0) \\
&= \log s \circ g(x) - (1-y) g(x) - \frac{1}{2}(x-\mu_0)^T \Sigma_0^{-1}(x-\mu_0)
\end{aligned}
\tag{7}
$$

Then the gradient of $f(x)$ is given by:

$$
\begin{aligned}
J(x) &= \frac{\partial f}{\partial x} \\
&= \left(1 - s \circ g(x)\right)\frac{\partial g}{\partial x} - (1-y)\frac{\partial g}{\partial x} - \Sigma_0^{-1}(x-\mu_0) \\
&= \frac{\partial g}{\partial x} - s \circ g(x)\frac{\partial g}{\partial x} - \frac{\partial g}{\partial x} + y\frac{\partial g}{\partial x} - \Sigma_0^{-1}(x-\mu_0) \\
&= \left(y - s \circ g(x)\right)\frac{\partial g}{\partial x} - \Sigma_0^{-1}(x-\mu_0)
\end{aligned}
\tag{8}
$$

And its Hessian can be approximated as:

$$
\begin{aligned}
H(x) &= \frac{\partial^2 f}{\partial x^2} \\
&= \left(y - s \circ g(x)\right)\frac{\partial g}{\partial x} - \Sigma_0^{-1}(x-\mu_0) \\
&= -s \circ g(x)\left(1 - s \circ g(x)\right)\frac{\partial g}{\partial x}\frac{\partial g}{\partial x}^T + \left(y - s \circ g(x)\right)\frac{\partial^2 g}{\partial x^2} - \Sigma_0^{-1} \\
&\approx -s \circ g(x)\left(1 - s \circ g(x)\right)\frac{\partial g}{\partial x}\frac{\partial g}{\partial x}^T - \Sigma_0^{-1}
\end{aligned}
\tag{9}
$$

if the mapping $g(x)$ is weakly nonlinear (and thus its higher-order derivative tends to zero).

Note that the first Gauss-Newton iteration thus writes:

$$
\mu \leftarrow \mu_0 - H(\mu_0)^{-1} J(\mu_0) = \left[ s \circ g(\mu_0)\left(1 - s \circ g(\mu_0)\right)\frac{\partial g}{\partial x}\frac{\partial g}{\partial x}^T + \Sigma_0^{-1} \right]^{-1} \frac{\partial g}{\partial x}\left(y - s \circ g(\mu_0)\right)
$$

if one initializes the optimizer with the prior mean (i.e., $x^* = \mu_0$)!

## III. Neuro-Imaging

**III.1 Research Ethics, Sample, and Exclusion Criteria**. The neuroimaging experiment (Experiment 5) was approved by the Psychology Research Ethics Board of Leiden (CEP19-0617/350) and the Leids Universitair Medisch Centrum Medical Ethics Committee (NL43120.058.13). We recruited 50 participants between the ages of 18 and 35 with normal or corrected to normal vision who had a good command of written and spoken English and who adhered to normal safety guidelines for MRI research (i.e., no metal implants or recently applied tattoos).

**III.2 Experimental Procedures and Tasks**. All neuroimaging was conducted at the Leiden Institute for Brain and Cognition 3T Philips Achieva MRI scanner at the Leids Universitair Medisch Centrum. On arrival participants were escorted to a private interview room where they would read the information brochure and sign the informed consent. After this, a researcher would verbally go through a medical safety checklist in order to ensure that the participant could enter the MRI scanner safely. After the medical safety checklist, participants completed the instructions for the tasks. The instructions were presented on a laptop and included test questions to ensure that participants understood the instructions fully. The participant was only allowed to proceed once they had answered each test question correctly. A researcher was always right outside the door in case they had any clarification questions. After participants had completed the instructions for the task, they were escorted into the MRI scanner room and put supine into the scanner, at which point the experimental tasks began.

**III.3 Data Acquisition and Pre-processing.** Neuroimaging was performed using a standard whole-head coil. Participants completed four runs, during which 400 T2*-weighted whole-brain echo-planar images (EPIs) were collected (TR = 2.2 s; TE = 30 ms, flip angle = 80°, 38 transverse slices, 2.75 × 2.75 × 2.75 mm +10% interslice gap). The first five dummy scans were discarded to allow for equilibration of T1 saturation effects. After each functional run, a B0 field map was acquired. Additionally, a 3-D T1-weighted scan was acquired (TR = 9.8 ms; TE = 4.6 ms, flip angle = 8°, 140 slices, 1.166 × 1.166 × 1.2 mm, FOV = 224.000 × 177.333 × 168.000).

Neuro-imaging data were preprocessed using FMRIPREP version 1.0.8 (16), a Nipype (17) based tool. Each T1w (T1-weighted) volume was corrected for INU (intensity non-uniformity) using N4BiasFieldCorrection v2.1.0 (18) and skull-stripped using antsBrainExtraction.sh v2.1.0 (using the OASIS template). Brain surfaces were reconstructed using recon-all from FreeSurfer v6.0.1 (19), and the brain mask estimated previously was refined with a custom variation of the method to reconcile ANTs-derived and FreeSurfer-derived segmentations of the cortical gray-matter of Mindboggle (20). Spatial

normalization to the ICBM 152 Nonlinear Asymmetrical template version 2009c (21) was performed through nonlinear registration with the antsRegistration tool of ANTs v2.1.0 (22), using brain-extracted versions of both T1w volume and template. Brain tissue segmentation of cerebrospinal fluid (CSF), white-matter (WM) and gray-matter (GM) was performed on the brain-extracted T1w using fast (FSL v5.0.9) (23).

Functional data was motion corrected using mcflirt (FSL v5.0.9) (24). This was followed by co-registration to the corresponding T1w using boundary-based registration (25) with 9 degrees of freedom, using bbregister (FreeSurfer v6.0.1). Motion correcting transformations, BOLD-to-T1w transformation and T1w-to-template (MNI) warp were concatenated and applied in a single step using antsApplyTransforms (ANTs v2.1.0) using Lanczos interpolation. Physiological noise regressors were extracted applying CompCor (26). Principal components were estimated for the two CompCor variants: temporal (tCompCor) and anatomical (aCompCor). A mask to exclude signal with cortical origin was obtained by eroding the brain mask, ensuring it only contained subcortical structures. Six tCompCor components were then calculated including only the top 5% variable voxels within that subcortical mask. For aCompCor, six components were calculated within the intersection of the subcortical mask and the union of CSF and WM masks calculated in T1w space, after their projection to the native space of each functional run. Frame-wise displacement (27) was calculated for each functional run using the implementation of Nipype. Many internal operations of FMRIPREP use Nilearn (28), principally within the BOLD-processing workflow. For more details of the pipeline, see: http://fmriprep.readthedocs.io/en/latest/workflows.html.

**III.4 General Linear Model and Supplementary Results.** Preprocessed functional data was then analyzed with FSL (Oxford Centre for Functional MRI of the Brain (FMRIB) Software Library; www.fmrib.ox.ac.uk/fsl). For all general linear models (GLMs), at the first level (within participants within runs), each participants' blood oxygen level dependent (BOLD) data was spatially smoothed with 5mm FWHM gaussian kernel, high pass temporal filtered, film pre-whitened, and convolved with the canonical double gamma hemodynamic response function. We then constructed the following GLMs:

GLM1 tested for effects of our BPL model's choice prediction error (both components in aggregate) as well as expected utility (both expected gain and inequality aversion in aggregate). GLM1 contained the following regressors: "responder": the time-phase when the shape representing the different responder population was presented; "expected utility": the "responder" regressor modulated by the expected utility of our BPL model and orthogonalized with respect to "responder"; "feedback": the time-phase when the response of the opponent was presented to the subject; "choice prediction error": "feedback" modulated by the prediction error from our BPL model, orthogonalized with respect to "feedback".

GLM2 tested for effects of our BPL model's choice prediction error with the separate components (choice prediction and actual outcome) as separate regressors. GLM2 contained the following regressors: "feedback": the time-phase when the response of the opponent was presented to the subject; "choice prediction": "feedback" modulated by the predicted likelihood of offer acceptance, as dictated by the parameters of our BPL model, orthogonalized with respect to "feedback"; and "outcome", "feedback" modulated by whether the offer was accepted (denoted with 1) or rejected (denoted with 0), orthogonalized with respect to "feedback". A true prediction error should be expressed as a positive correlation with the outcome, and a negative correlation with the prediction thereof (29, 30).

GLM3 tested for effects of a reward prediction error—derived from our BPL model's choice prediction error—with the separate components (reward prediction and actual payoff) as separate regressors. GLM3 contained the following regressors: "feedback": the time-phase when the response of the opponent was presented to the subject; "reward prediction": "feedback" modulated by the predicted payoff given the choice prediction derived from the parameters of our BPL model, orthogonalized with respect to "feedback"; and "payoff", "feedback" modulated by the actual payoff received, orthogonalized with respect to "feedback".

Finally, GLM4 tested for effects of our BPL model's expected utility parameter with separate components: expected gain and (in the social condition) inequality aversion. GLM4 contained the following regressors: "responder": the time-phase when the shape representing the different responder population was presented; "expected gain": the "responder" regressor modulated by the expected gain of our BPL model and orthogonalized with respect to "responder"; "inequality aversion" (only in the social condition): the "responder" regressor modulated by the inequality aversion of the given offer ((endowment – offer)^2); "feedback": the time-phase when the response of the opponent was presented to the subject; "choice prediction error": "feedback" modulated by the prediction error from our BPL model, orthogonalized with respect to "feedback". Note that because each regressor was z-scored within each run within each participant (see below), we did not need to include the subject-specific inequality aversion weight.

Importantly, and as recommended best practice (31), all parametric regressors were normalized by z-scoring the weighted values within runs and participants. Therefore, every participant's parametric regressor had a mean of 0 and a standard deviation of 1. We also included temporal derivatives for all of these regressors, six motion parameters (three rotation and three translation), framewise displacement (32), and six anatomical principal components (26). Furthermore, analyses for all GLMs averaged within participants within runs at the first level of analysis, averaged within participants across runs at the second level of analysis—which is also where social/non-social contrasts were implemented—and across participants at

the third level of analysis. Significance was determined at the group level with FSL's FLAME 1 with standard cluster forming threshold of $Z > 3.1$ and cluster significance at $p < 0.01$. We utilized the default settings within FSL, which applies random field theory to implement family-wise error correction at the cluster level. Table S7-S11 present the significant results from our analysis concerning the latent parameters of our BPL model.

**Table S7**: Positive correlations of prediction error with neural activation

| Region | cluster size (voxels) | X (mm) | Y (mm) | Z (mm) | Z-stat max |
|---|---|---|---|---|---|
| R Precentral Gyrus | 2628 | 3 | -16.5 | 55.1 | 6.17 *** |
| PCC | 1070 | -5.25 | -55 | 18.8 | 6.46 *** |
| VMPFC | 339 | -2.5 | 63.2 | -5.4 | 6.23 *** |
| R Hipp | 165 | 19.5 | -13.8 | -23.5 | 5.45 *** |
| L Post Cent Gyr | 154 | -63 | -8.25 | 18.8 | 4.51 *** |
| R LOC | 137 | 27.8 | -82.5 | 46 | 5.17 *** |
| L Hipp | 112 | -24.5 | -22 | -17.5 | 5.58 *** |
| L LOC | 97 | -38.2 | -85.2 | 37 | 4.26 *** |
| L Frontal Pole | 93 | -49.2 | 44 | 9.73 | 5.44 *** |
| C Opercular Cortex | 78 | -38.2 | -2.75 | 18.8 | 5.46 *** |
| Occip Fusiform | 76 | -16.2 | -77 | -11.4 | 3.93 *** |
| ITG | 69 | -57.5 | -55 | -14.5 | 4.85 ** |
| L SFG | 66 | -24.5 | 30.2 | 49.1 | 5.03 ** |
| L OFC | 66 | -38.2 | 38.5 | -11.4 | 5.17 ** |
| R LOC | 57 | 44.2 | -63.2 | 3.68 | 4.75 ** |
| L Occip Pole | 48 | -13.5 | -93.5 | 24.9 | 4.28 * |
| L LOC | 47 | -54.8 | -74.2 | 12.8 | 4.74 * |
| L Caudate | 39 | -19 | 5.5 | 24.9 | 4.14 * |
| L Occip Pole | 37 | -24.5 | -85.2 | 46 | 4.23 * |
| R Precentral Gyrus | 29 | 22.2 | -19.2 | 64.2 | 4.04 * |
| R OFC | 26 | 27.8 | 38.5 | -11.4 | 4.18 * |

*Note.* All statistics are corrected for multiple comparisons using FLS's FLAME 1 with standard cluster forming threshold of $Z > 3.1$ and cluster significance at $p < 0.01$, *** $p < 0.001$, ** $p < 0.01$, * $p < 0.05$, # $p < 0.10$.

**Table S8**: Negative correlations of prediction error with neural activation

| Region | cluster size (voxels) | X (mm) | Y (mm) | Z (mm) | Z-stat max |
|---|---|---|---|---|---|
| ACC/SFG | 1639 | 0.25 | 13.8 | 64.2 | 6.18 *** |
| R Insula/IFG | 1170 | 52.5 | 19.2 | -2.37 | 6.84 *** |
| R TPJ | 524 | 60.8 | -55 | 30.9 | 5.58 *** |
| L Insula/IFG | 402 | -38.2 | 22 | -8.42 | 7.18 *** |
| R STG | 340 | 55.2 | -22 | -8.42 | 7.23 *** |
| L TPJ | 184 | -63 | -46.8 | 37 | 5.3 *** |
| R Caudate | 123 | 11.2 | 13.8 | 12.8 | 5.01 *** |
| L Caudate | 63 | -13.5 | 2.75 | 9.73 | 4.59 ** |
| L STG | 60 | -52 | -27.5 | -5.4 | 5.01 ** |
| PCC | 35 | 5.75 | -33 | 3.68 | 4.1 * |
| Temporal Pole | 33 | 52.5 | 8.25 | -20.5 | 4.5 * |
| L DLPFC | 30 | -41 | 22 | 37 | 4.01 * |
| Precuneus | 29 | 0.25 | -77 | 12.8 | 4.37 * |
| L Frontal Pole | 29 | -30 | 57.8 | 21.8 | 3.86 * |
| Precuneus | 29 | -10.8 | -77 | 12.8 | 4.02 * |

*Note.* All statistics are corrected for multiple comparisons using FLS's FLAME 1 with standard cluster forming threshold of $Z > 3.1$ and cluster significance at $p < 0.01$, *** $p < 0.001$, ** $p < 0.01$, * $p < 0.05$, # $p < 0.10$.

**Table S9**: Positive correlations of expected utility with neural activation

| Region | cluster size (voxels) | X (mm) | Y (mm) | Z (mm) | Z-stat max |
|---|---|---|---|---|---|
| VMPFC | 111 | 5.75 | 55 | -11.4 | 4.79 *** |
| VS | 51 | 0.25 | 16.5 | -5.4 | 4.53 * |
| STG | 32 | 63.5 | 5.5 | -5.4 | 4.34 * |

*Note.* All statistics are corrected for multiple comparisons using FLS's FLAME 1 with standard cluster forming threshold of $Z > 3.1$ and cluster significance at $p < 0.01$, *** $p < 0.001$, ** $p < 0.01$, * $p < 0.05$, # $p < 0.10$.

**Table S10**: Negative correlations of expected utility with neural activation

| Region | cluster size (voxels) | X (mm) | Y (mm) | Z (mm) | Z-stat max |
|---|---|---|---|---|---|
| Precuneus | 1775 | -2.5 | -74.2 | 55.1 | 5.58 *** |
| R Occip Fusiform | 703 | 25 | -77 | -8.42 | 6.19 *** |
| ACC/SFG | 385 | 5.75 | 38.5 | 49.1 | 5.37 *** |
| L Temp Fusiform | 338 | -38.2 | -46.8 | -23.5 | 5.19 *** |
| R DLPFC | 303 | 47 | 11 | 30.9 | 5.63 *** |
| L IFC | 246 | -41 | 2.75 | 24.9 | 4.96 *** |
| L OFC | 218 | -30 | 30.2 | -5.4 | 5.59 *** |
| L Thalamus | 156 | -2.5 | -24.8 | 9.73 | 4.53 *** |
| R Insula | 144 | 33.2 | 22 | 3.68 | 4.63 *** |
| L DLPFC | 122 | -35.5 | -2.75 | 64.2 | 5.11 *** |
| L Caudate | 64 | -10.8 | 11 | 9.73 | 5.43 ** |
| L Frontal Pole | 53 | -32.8 | 60.5 | 3.68 | 3.74 ** |
| R DLPFC | 45 | 44.2 | 5.5 | 55.1 | 4.08 * |
| SFG | 32 | 19.5 | 16.5 | 67.2 | 3.96 * |
| R Frontal Pole | 29 | 41.5 | 55 | -5.4 | 4.01 * |
| ACC | 26 | -2.5 | -13.8 | 27.9 | 3.86 * |

*Note*. All statistics are corrected for multiple comparisons using FLS's FLAME 1 with standard cluster forming threshold of $Z > 3.1$ and cluster significance at $p < 0.01$, *** $p < 0.001$, ** $p < 0.01$, * $p < 0.05$.

**Table S11**: Positive correlations of inequality aversion with neural activation

| Region | cluster size (voxels) | X (mm) | Y (mm) | Z (mm) | Z-stat max |
|---|---|---|---|---|---|
| L Occip Fusiform | 1452 | -13.5 | -82.5 | -5.4 | 6.14 *** |
| L OFC | 93 | -32.8 | 24.8 | -17.5 | 4.39 *** |
| R Insula | 77 | 30.5 | 24.8 | -5.4 | 4.99 *** |
| Brain Stem | 49 | 11.2 | -24.8 | -11.4 | 4.47 ** |
| R Caudate | 42 | 8.5 | 16.5 | 0.65 | 4.88 ** |
| L VS | 35 | -5.25 | 11 | -5.4 | 4.22 ** |
| R Occip Fusiform | 35 | 38.8 | -71.5 | -14.5 | 3.97 ** |

*Note*. All statistics are corrected for multiple comparisons using FLS's FLAME 1 with standard cluster forming threshold of $Z > 3.1$ and cluster significance at $p < 0.01$, *** $p < 0.001$, ** $p < 0.01$, * $p < 0.05$.

### III.5 Region of Interest Analysis

For both GLM2 and GLM3 we utilized a region of interest (ROI) approach. We selected the ventral striatum (VS) as an ROI due it it's consistent association with reward prediction errors (33). In order to avoid biasing our results in favor of our choice prediction error GLM (GLM2), we obtained our VS mask independently from Neurosynth (34) with the search term "ventral striatum", and thresholded at 9. We extracted the

parameter estimates of each participant from with this VS mask, and then submitted the resulting values to paired *t*-tests (see Main Text, **Fig 7B**).

Due to the robust activations found in nodes of the punishment and reward networks, we next conducted analyses with ROI's obtained from these previous analyses. Specifically, we isolated regions identified in GLM1 (see section **III.4**) that we reasoned could likewise exhibit differential activations with respect to the different components of our expected utility function—i.e., separately for expected gain and (in the social condition) inequality aversion (see Main Text, **Fig 3A**).

From the reward network we selected the ventromedial prefrontal cortex (VMPFC) and ventral striatum (VS), which we hypothesized would differentiate between the different components of our expected utility parameter due to their consistent involvement in anticipatory valuation – the VMPFC in particular (14). From the punishment network we selected the dorsal anterior cingulate (dACC) and anterior insula, as these nodes have been demonstrated to be the most robustly involved in the processing of punishment, including punishment in the form of offer rejections in the ultimatum game (14, 35).

We took the average BOLD activation within each ROI for each participant for both expected gain and inequality aversion, and submitted each participant's averaged BOLD response within the given ROI to one-sample *t*-tests against 0. Results are presented in **Table S12**.

**Table S12**: *t*-tests on components of expected utility in ROIs

| | *t*-stats | | | |
|---|---|---|---|---|
| | VMPFC | VS | dACC | Ant. Insula |
| Non-social Expected Gain | 2.971 ** | 3.350 ** | -5.609 *** | -5.288 *** |
| Social Expected Gain | 3.245 ** | 5.237 *** | -4.768 *** | -7.238 *** |
| Inequality aversion | 0.504 | -0.084 | 2.242 * | 4.829 *** |
| Observations | 49 | 49 | 49 | 49 |

*Note*. All *t*-stats contrasts are against 0. *** $p < 0.001$, ** $p < 0.01$, * $p < 0.05$, # $p < 0.10$ (two-tailed tests).

### III.6 Multivariate Analysis and Supplementary Results

We employed multi-voxel pattern analysis (MVPA) to examine patterns of neural activity during both the decision and feedback time-phases in order to detect subtle differences in neural processing between the social and non-social conditions. For each subject we fit a general linear model (GLM) to each trial time-locked to the time-phase of interest (i.e., for both decision and feedback time-phases). This resulted in a

single parameter estimate for each trial during each epoch of interest. For each subject, we concatenated these parameter estimates together to create a single image file with 288 volumes, each volume corresponding to the parameter estimate of a given trial. We then applied a 27-voxel searchlight procedure with a linear discriminant analysis (LDA) classifier. A searchlight acts as a traveling region of interest used to detect spatially contiguous patterns of activation specific to functional neural structures (36). Each subject completed two social and two non-social functional runs, and we therefore conducted a leave-two-runs-out cross-validation procedure, in which our LDA classifier was trained on two runs (one social and one non-social), and then tested on the two independent left-out runs. This resulted in a single accuracy map for each subject. The resulting accuracy maps were then concatenated together and tested for significance with Monte Carlo boot-strapping with 10,000 permutations with threshold-free cluster enhancement (TFCE) (37), family-wise error correct (FWE-corrected) at the whole-brain level with threshold of $Z > 1.6449$ ($p < 0.05$), implemented in the CoSMoMVPA MATLAB package (4). To maximize statistical sensitivity, we created null datasets for significance testing by permuting condition labels. Specifically, for each subject we permuted the labels indicating which condition each volume of their image file belonged to, and ran the searchlight on said permuted image. This process was repeated 100 times for each subject as recommended by Stelzer and colleagues (27) resulting in 100 "null" accuracy maps, representing results from randomized data. These data were used as the null data in the group level TFCE analysis.

**Table S13**: Social vs. non-social during decision-making

| Region | cluster size (voxels) | X (mm) | Y (mm) | Z (mm) | Z-stat max |
|---|---|---|---|---|---|
| Occip Pole | 2342 | 3 | -88 | 6.7 | 3.72 *** |
| PCC/precuneus | 1353 | 0.25 | -19.2 | 27.9 | 3.35 *** |
| R IFG | 1178 | 55.2 | 11 | 24.9 | 3.35 *** |
| R SFG | 133 | 27.8 | 2.75 | 55.1 | 2.66 ** |
| dACC | 129 | -5.25 | 0 | 67.2 | 2.18 * |
| R TPJ | 41 | 49.8 | -41.2 | 58.1 | 1.98 * |
| L Putamen | 32 | -32.8 | -2.75 | -5.4 | 2.24 * |
| L Insula | 17 | -32.8 | 16.5 | -11.4 | 1.9 * |
| L STS | 17 | -60.2 | -52.2 | 15.8 | 2.05 * |
| L TPJ | 14 | -54.8 | -44 | 61.2 | 2.1 * |
| VS | 9 | -8 | 8.25 | -8.42 | 1.82 * |
| L STG | 8 | -46.5 | -41.2 | 9.73 | 1.94 * |
| R TPJ | 7 | 63.5 | -38.5 | 46 | 2.11 * |
| R Post Cen Gyr | 6 | 36 | -30.2 | 52.1 | 1.73 * |
| L LOC | 5 | -35.5 | -77 | -2.37 | 1.67 * |
| R LOC | 5 | 38.8 | -60.5 | 40 | 1.69 * |

*Note.* All statistics are FWE corrected for multiple comparisons using threshold free cluster enhancement(37) as implemented in CoSMoMVPA(4), with threshold of Z > 1.6449 ($p < 0.05$). *** $p < 0.001$, ** $p < 0.01$, * $p < 0.05$, # $p < 0.10$.

**Table S14**: Social vs. non-social during feedback

| Region | cluster size (voxels) | X (mm) | Y (mm) | Z (mm) | Z-stat max |
|---|---|---|---|---|---|
| Precuneus | 102 | 3 | -63.2 | 24.9 | 2.46 ** |
| Occip Pole | 82 | 11.2 | -96.2 | 24.9 | 2.45 ** |
| dACC | 10 | -5.25 | 19.2 | 33.9 | 1.95 * |
| Occip Pole | 7 | -5.25 | -99 | -5.4 | 1.88 * |
| L LOC | 6 | -32.8 | -88 | 18.8 | 1.83 * |
| Lingual Gyr | 5 | -13.5 | -77 | -2.37 | 1.74 * |
| Occip Pole | 5 | 8.5 | -90.8 | 9.73 | 1.74 * |

*Note.* All statistics are FWE corrected for multiple comparisons using threshold free cluster enhancement(37) as implemented in CoSMoMVPA(4), with threshold of Z > 1.6449 ($p < 0.05$). *** $p < 0.001$, ** $p < 0.01$, * $p < 0.05$, # $p < 0.10$.

## IV. Experimental Instructions.

**IV.1 Screenshots of the Instructions and Stimuli for Behavioral Experiments.** This section contains screenshots of the instructions provided to participants for our behavioral experiments as well as screenshots of experimental stimuli. Because instructions and stimuli for laboratory and online behavioral experiments were almost identical, only one set of screenshots are provided.

# Introduction

## Instructions

Please enter your Prolific ID:

What is your age?

---------

What is your gender?

---------

Please read the following very carefully.

In this experiment, you will be completing four different tasks. Instructions for each task will be provided separately.

One random trial from each of these four tasks will be chosen to calculate the extra money you earn. This means that the decisions you make on each task will affect your extra payout. You should therefore read the instructions very carefully.

### Ultimatum Task

In the ultimatum task , you will be acting as the so-called **proposer**. This means that you will get a 20 MU monetary unit (MU) endowment **(20 MU = €2.50)**. With this endowment, you will make a take-it-or-leave-it offer to another person – the responder.

The responder can accept your offer. In this case both you and the responder keep whatever money you have proposed.

The responder can also reject your offer. In this case, both you and the responder receive 0 MU.

As the proposer you have the following 21 options on how to divide the 20 MU between the you and the responder.

0 MU for the responder (you keep 20 MU)
1 MU for the responder (you keep 19 MU)
2 MU for the responder (you keep 18 MU)
3 MU for the responder (you keep 17 MU)
4 MU for the responder (you keep 16 MU)
5 MU for the responder (you keep 15 MU)
6 MU for the responder (you keep 14 MU)
7 MU for the responder (you keep 13 MU)
8 MU for the responder (you keep 12 MU)
9 MU for the responder (you keep 11 MU)
10 MU for the responder (you keep 10 MU)
11 MU for the responder (you keep 9 MU)
12 MU for the responder (you keep 8 MU)
13 MU for the responder (you keep 7 MU)
14 MU for the responder (you keep 6 MU)
15 MU for the responder (you keep 5 MU)
16 MU for the responder (you keep 4 MU)
17 MU for the responder (you keep 3 MU)
18 MU for the responder (you keep 2 MU)
19 MU for the responder (you keep 1 MU)
20 MU for the responder (you keep 0 MU)

You can only make one offer to the responder. Only after you make an offer, you will learn whether it was accepted or rejected.

### Human and computer conditions

You will be interacting in two different conditions: a **human**, and a **computer**.

In the human condition, you will be making offers to other real individuals. These individuals have already stated, for every possible offer, whether they would accept or reject it.

When you make your decision, you will not know what offer the current responder would accept. However, after you make your decision, you will learn about whether your current responder accepted your offer or not.

After you are finished with this experiment, you and these individuals will be paid based on the offers that you decided to make and – of course – whether they accepted or rejected your offer.

**This means that the offers that you make will not only affect your own payoff but also the payoff of other individuals in the human condition.**

Yet, there is also another condition: The computer condition.

In the computer condition, you will be making offers to the computer instead of a real human. The computer is programmed such that it matches the actual decisions of human responders.

In other words, you will be interacting with a computer program that is programmed to accept or reject offers in the same way as real individuals in the human condition do. **However, in this condition your offers will not affect the payment of other individuals but only your own payoff.**

Please answer the following questions. These questions serve to check your comprehension of the task. If you are unsure, please re-read the instructions.

You will only be allowed to continue with the study if you answer these questions correctly.

The payout of another individual will be affected by my offers in the computer condition:

- ○ TRUE
- ○ FALSE

The payout of another individual will be affected by my offers in the human condition:

- ○ TRUE
- ○ FALSE

If the responder rejects my offer, both I and the responder keep the proposed amount:

- ○ TRUE
- ○ FALSE

If the responder accepts my offer, both I and the responder keep the proposed amount:

- ○ TRUE
- ○ FALSE

Next

# Introduction

## Ultimatum Task

In the following ultimatum task, you will still be playing in both a human and a computer condition.

In both conditions, you will be interacting with multiple responders (either human or computer, depending on the condition) over multiple rounds who come from **3 different groups.**

In the Human condition, individuals from these 3 groups received different starting endowments.

For example, responders from one group may have received a starting endowment of 15 MU to begin with. This means, you start with 20 MU and a responder from this group starts with 15 MU. Then you make an offer to the responder from this group. If the responder accepts your offer, he/she keeps the starting endowment plus the amount that was offered by you. If the responder rejects your offer, he/she only keeps the starting endowment and you receive 0 MU.

In the Computer condition, you will also be playing against 3 different responder groups. Hence, the responses you get are programmed to mimic the decision-making of individuals from the 3 different groups who did receive different starting endowments. As mentioned above, the only difference in the Computer condition is, that your offers will not affect the payment of other human individuals but only your own payoffs.

Importantly, how much each group received as a starting endowment will remain unknown to you. But you will be able to identify to which group a responder belongs to through different colors.

To summarize:

> In each round you will be paired to one responder.
>
> You will learn to which group this responder belongs to by a color.
>
> The responders from different groups differ in how many MU they received as a starting endowment. This starting endowment is theirs to keep regardless of whether they accept or reject your offer.
>
> You will then receive 20 MU and have to make an offer on how to split these 20 MU between you and the responder.
>
> You will then learn whether the responder accepted or rejected your offer. If he/she accepts your offer, both of you receive the offered amount. If he/she rejects your offer, the 20 MU are gone and both of you receive 0 MU.
>
> In the Human condition, you interact with real responders. Your decisions (and the responder's decision to accept or reject your offers) therefore will not only impact your own payoff but also the payoff of another real person.
>
> In the Computer condition, responders are programmed such that they mimic the decisions of real humans. Yet, in this condition, the outcome of your decision only affects your own payoff.

Please answer the following questions. These questions serve to check your comprehension of the task. If you are unsure, please re-read the instructions.

You will only be allowed to continue with the study if you answer these questions correctly.

The payout of another individual will be affected by my offers in the computer condition:

- ○ TRUE
- ○ FALSE

The payout of another individual will be affected by my offers in the human condition:

- ○ TRUE
- ○ FALSE

If the responder rejects my offer, both I and the responder keep the proposed amount:

- ○ TRUE
- ○ FALSE

If the responder accepts my offer, both I and the responder keep the proposed amount:

- ○ TRUE
- ○ FALSE

In the human condition, different colors indicate:

- ○ Randomly chosen responders
- ○ Groups of responders who received different starting endowments
- ○ Groups of responders from different academic backgrounds
- ○ All of the above

In the computer condition, different colors indicate:

- ○ Random computer generate lotteries
- ○ Computer responses programmed to mimic responders who received different starting endowments
- ○ Computer responses programmed to mimic responders from different academic backgrounds
- ○ All of the above

Please ask the researcher if you have any questions

Next

# **Human** condition

You are playing against a responder from group

You have **20 MU**. Enter the amount that you want to offer to the responder.

How much would you like to offer?

○ 0 MU ○ 1 MU ○ 2 MU ○ 3 MU ○ 4 MU ○ 5 MU ○ 6 MU ○ 7 MU ○ 8 MU ○ 9 MU ○ 10 MU ○ 11 MU
○ 12 MU ○ 13 MU ○ 14 MU ○ 15 MU ○ 16 MU ○ 17 MU ○ 18 MU ○ 19 MU ○ 20 MU

Next

Your offer of 13 MU was **ACCEPTED**

You therefore received **7 MU** on this trial.

The responder received **13 MU** on this trial.

Next

## **Computer** condition

You are playing against a responder from group

You have **20 MU**. Enter the amount that you want to offer to the responder.

How much would you like to offer?

○ 0 MU ○ 1 MU ○ 2 MU ○ 3 MU ○ 4 MU ○ 5 MU ○ 6 MU ○ 7 MU ○ 8 MU ○ 9 MU ○ 10 MU ○ 11 MU
○ 12 MU ○ 13 MU ○ 14 MU ○ 15 MU ○ 16 MU ○ 17 MU ○ 18 MU ○ 19 MU ○ 20 MU

Next

Your offer of 12 MU was **ACCEPTED**

You therefore received **8 MU** on this trial.

Next

# Introduction

## Instructions

After every 2 blocks of the ultimatum task, you will play a probability matching task in which you must guess how likely it is that a given offer will be accepted by a certain opponent. For example, we will ask how likely an offer of 5 will be accepted by an opponent from the green group, and you must answer on a scale from 0% to 100%.

Importantly, your performance on this task will also affect your extra payment. The closer your estimate of the offer's probability of acceptance is to the actual probability that the offer will be accepted, the higher your chances of earning extra money on this task. In other words, you should try to be as accurate as possible in your guesses in order to earn the most money on this task.

## Comprehension questions:

In the following task I will be asked:

- ○ How likely a given offer was to be accepted
- ○ What percentage of people would accept a given offer
- ○ How likely I would be to accept a given offer

My payment will be affected by my accuracy on this task:

- ○ correct
- ○ incorrect

Next

When you were making offers to a responder from

And you offered **14**.

How likely were they to accept the offer?

How likely is this offer to be accepted (in percent)?

92

Next

When you were making offers to a responder from

And you offered **3**.

How likely were they to accept the offer?

How likely is this offer to be accepted (in percent)?

75

Next

**IV.2 Screenshots of the Instructions and Stimuli for Neuroimaging Experiments.** In order to make our experiment fMRI compatible, we made some changes to the stimuli. Below are images from the fMRI compatible experiment.

# Introduction

## Instructions

Please read the following very carefully, and ask the researcher if you have any questions.

In this experiment, you will be completing 2 different tasks: the ultimatum task, and a probability matching task. One random trial from each of these tasks will be chosen to calculate the extra money you earn, therefore you will be paid out the extra amount earned on 4 trials. This means that the decisions you make on each task will affect your extra payout.

### Ultimatum Task

In the ultimatum task , you will be acting as the so-called **proposer**. This means that, on every trial, you will have a 20 MU monetary unit (MU) endowment **(20 MU = €2.50)**. With this endowment, you will make a take-it-or-leave-it offer to the other player – the responder. The responder will either accept your offer, in which case both you and the responder keep whatever money you have proposed, or reject the offer, in which case both you and the responder receive 0 MU MU for that trial. Both your identity, and that of the responder, will remain hidden.

As the proposer you have the following 21 options on how to divide the 20 MU MU between the you and the responder.

1. 0 MU for the responder (you keep 20 MU)
2. 1 MU for the responder (you keep 19 MU)
3. 2 MU for the responder (you keep 18 MU)
4. 3 MU for the responder (you keep 17 MU)
5. 4 MU for the responder (you keep 16 MU)
6. 5 MU for the responder (you keep 15 MU)
7. 6 MU for the responder (you keep 14 MU)
8. 7 MU for the responder (you keep 13 MU)
9. 8 MU for the responder (you keep 12 MU)
10. 9 MU for the responder (you keep 11 MU)
11. 10 MU for the responder (you keep 10 MU)
12. 11 MU for the responder (you keep 9 MU)
13. 12 MU for the responder (you keep 8 MU)
14. 13 MU for the responder (you keep 7 MU)
15. 14 MU for the responder (you keep 6 MU)
16. 15 MU for the responder (you keep 5 MU)
17. 16 MU for the responder (you keep 4 MU)
18. 17 MU for the responder (you keep 3 MU)
19. 18 MU for the responder (you keep 2 MU)
20. 19 MU for the responder (you keep 1 MU)
21. 20 MU for the responder (you keep 0 MU)

The responder can either accept or reject the offer.

### Social and non-social conditions

You will be interacting in two different conditions: a **social**, and a **non-social**.

In the social condition, you will be making offers to other individuals who have already stated whether they would accept or reject the offer that you are making. In other words, we asked individuals whether they would accept or reject every possible offer, and are using their responses in the current experiment. Therefore, you are confronted with real decisions of real people in response to your offers. After we have collected the data for this study, these individuals will be paid based on the offers that you make as well as the offers that they said they would accept. Importantly, we practice **no deception** in this study. The offers that you make will affect other individuals, and the responses that you receive in the social condition do reflect the decisions of other individuals.

In the non-social condition, you will be making offers to computer generated lotteries with probabilities programmed to match human decision-making. In other words, you will be interacting with a computer program that is programmed to accept or reject offers in a way similar to a human. *However, in this condition your offers will not affect the payment of other individuals.*

In both conditions, you will be interacting with individuals (either real or programmed, depending on the condition) who come from 3 different groups.

In the social condition, these individuals received different starting endowments which were fixed for each group. In other words, the different groups received different amounts of MU to start with on each trial in addition to the MU which you offer them.

For example, if one group received a starting endowment of 15 MU, then the total amount of MU on that trial is 35 MU: 20 MU from the proposer (you), and 15 MU from the responder. If the responder accepts your offer, he/she will keep the starting endowment plus the amount that was offered by you. If the responder rejects your offer, he/she will only keep the starting endowment.

In the non-social condition, you will also be playing against 3 different groups. Hence, the responses you get are programmed to mimic the decision-making of individuals from 3 different groups who did receive different starting endowments. However, in this condition your offers will not affect the payment of other individuals.

How much each group received as a starting endowment will remain unknown to you. But the different groups are all labeled with different shapes.

In the social condition, these are all **empty shapes**, and in the non-social condition, these are all **solid shapes**, Additionally, the condition will be at the bottom of the screen during each trial.

Please answer the following questions. These questions serve to check your comprehension of the task. If you are unsure, please

re-read the instructions.

You will only be allowed to continue with the study if you answer these questions correctly.

My payout depends on the behavior of other human individuals in both conditions:

- ○ TRUE
- ○ FALSE

My payout depends on the behavior of other individuals in the social condition:

- ○ TRUE
- ○ FALSE

The payout of another individual will be affected by my offers in both conditions:

- ○ TRUE
- ○ FALSE

The payout of another individual will be affected by my offers in the social condition:

- ○ TRUE
- ○ FALSE

If the responder rejects my offer, both I and the responder keep the proposed amount:

- ○ TRUE
- ○ FALSE

If the responder accepts my offer, both I and the responder keep the proposed amount:

- ○ TRUE
- ○ FALSE

A solid shape indicates:

- ○ SOCIAL
- ○ NON-SOCIAL

An empty shape indicates:

- ○ SOCIAL
- ○ NON-SOCIAL

In the social condition, the different shapes represent:

- ○ Randomly chosen responders
- ○ Groups of responders who received different starting endowments
- ○ Groups of responders from different academic backgrounds
- ○ All of the above

In the non-social condition, the different shapes represent:

- ○ Random computer generate lotteries
- ○ Computer responses programmed to mimic responders who received different starting endowments
- ○ Computer responses programmed to mimic responders from different academic backgrounds
- ○ All of the above

Please ask the researcher if you have any questions

Next

opponent from

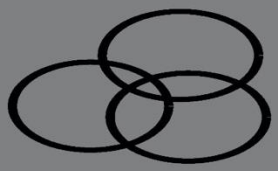

non-social

Your offer

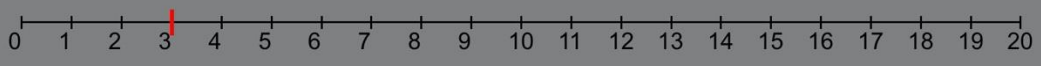

REJECTED

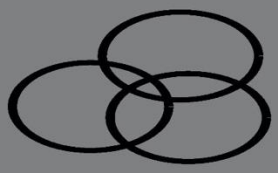

You receive 0

opponent from

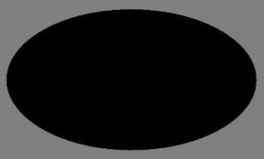

social

Your offer

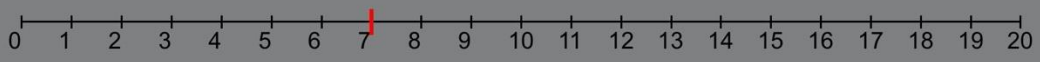


ACCEPTED

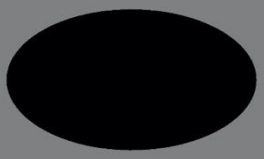

You receive 13

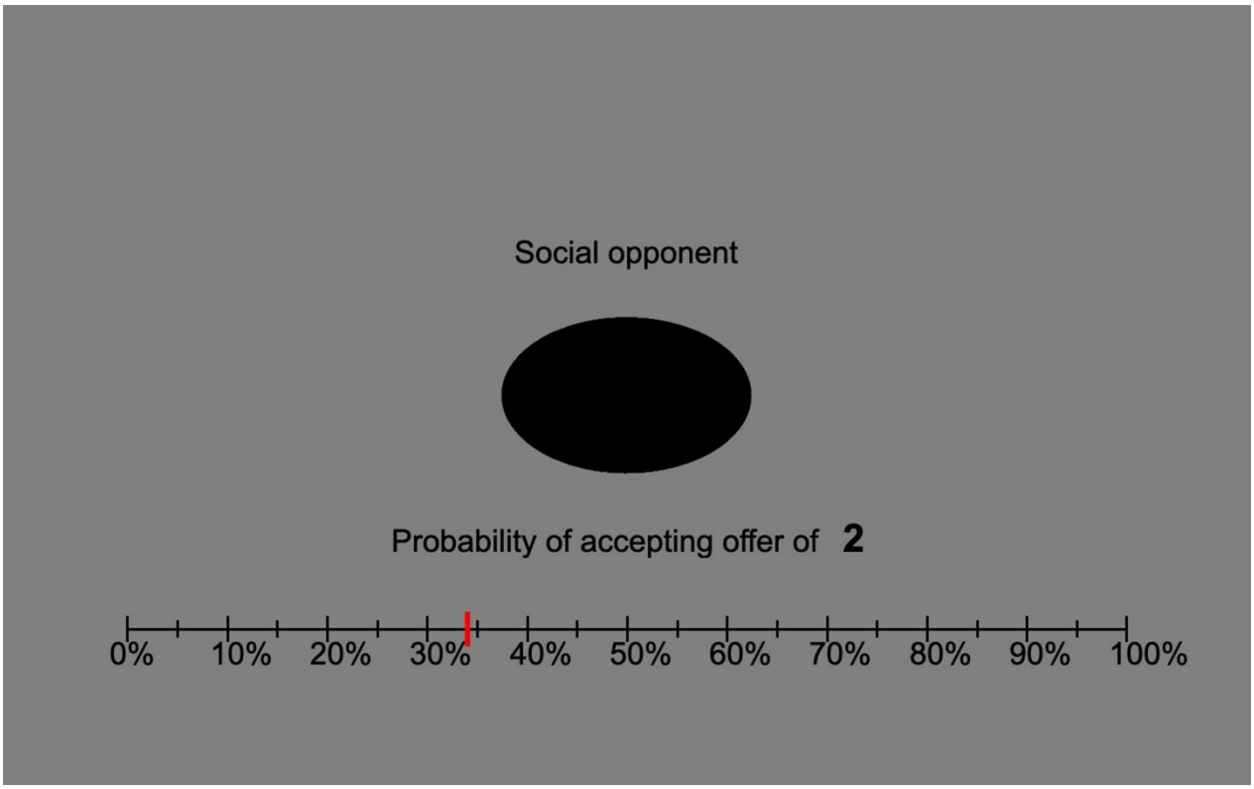
Social opponent
Probability of accepting offer of 2
0%
10%
20%
30%
40%
50%
60%
70%
80%
90%
100%

**References**


1. P. R. Blake, *et al.*, The ontogeny of fairness in seven societies. *Nature* **528**, 258–261 (2015).

2. J. Henrich, *et al.*, "Economic man" in cross-cultural perspective: behavioral experiments in 15 small-scale societies. *Behav. Brain Sci.* **28**, 795–815; discussion 815-55 (2005).

3. H. Oosterbeek, R. Sloof, G. van de Kuilen, Cultural differences in ultimatum experiments: Evidence from a meta-analysis. *Exp. Econ.* **7**, 171–188 (2004).

4. N. N. Oosterhof, A. C. Connolly, J. V Haxby, CoSMoMVPA: Multi-Modal Multivariate Pattern Analysis of Neuroimaging Data in Matlab/GNU Octave. *Front. Neuroinform.* **10** (2016).

5. M. Lebreton, *et al.*, Two sides of the same coin: Monetary incentives concurrently improve and bias confidence judgments. *Sci. Adv.* **4**, 1–14 (2018).

6. K. H. Schlag, J. Tremewan, J. J. van der Weele, A penny for your thoughts: a survey of methods for eliciting beliefs. *Exp. Econ.* **18**, 457–490 (2015).

7. V. L. Smith, J. M. Walker, Monetary rewards and decision cost in experimental economics. *Econ. Inq.* **31**, 245–261 (1993).

8. D. Bates, M. Mächler, B. M. Bolker, S. C. Walker, Fitting linear mixed-effects models using lme4. *J. Stat. Softw.* **67**, 1–48 (2015).

9. The R Development Core Team, R: A language and environment for statistical computing. *ISBN 3-900051-07-0* (2017).

10. C. Dave, C. C. Eckel, C. A. Johnson, C. Rojas, Eliciting risk preferences: When is simple better? *J. Risk Uncertain.* **41**, 219–243 (2010).

11. N. D. Daw, Trial-by-trial data analysis using computational models. *Decis. Making, Affect. Learn. Atten. Perform. XXIII*, 1–26 (2011).

12. R. H. Byrd, P. Lu, J. Nocedal, C. Zhu, A Limited Memory Algorithm for Bound Constrained Optimization. *SIAM J. Sci. Comput.* **16**, 1190–1208 (1995).

13. R. C. Wilson, A. G. Collins, Ten simple rules for the computational modeling of behavioral data. *Elife* **8** (2019).

14. S. Palminteri, M. Pessiglione, Opponent brain systems for reward and punishment learning: Causal evidence from drug and lesion studies in humans. *Decis. Neurosci. An Integr. Perspect.*, 291–303 (2017).

15. J. Daunizeau, V. Adam, L. Rigoux, VBA: A Probabilistic Treatment of Nonlinear Models for Neurobiological and Behavioural Data. *PLoS Comput. Biol.* **10** (2014).

16. O. Esteban, *et al.*, fMRIPrep: a robust preprocessing pipeline for functional MRI. *Nat. Methods* (2019) https:/doi.org/10.1038/s41592-018-0235-4.

17. K. Gorgolewski, *et al.*, Nipype: A flexible, lightweight and extensible neuroimaging data processing framework in Python. *Front. Neuroinform.* (2011) https:/doi.org/10.3389/fninf.2011.00013.

18. N. J. Tustison, *et al.*, N4ITK: Improved N3 bias correction. *IEEE Trans. Med. Imaging* (2010) https:/doi.org/10.1109/TMI.2010.2046908.

19. A. M. Dale, B. Fischl, M. I. Sereno, Cortical surface-based analysis: I. Segmentation and surface reconstruction. *Neuroimage* (1999) https:/doi.org/10.1006/nimg.1998.0395.

20. A. Klein, *et al.*, Mindboggling morphometry of human brains. *PLoS Comput. Biol.* (2017) https:/doi.org/10.1371/journal.pcbi.1005350.

21. V. Fonov, A. Evans, R. McKinstry, C. Almli, D. Collins, Unbiased nonlinear average age-appropriate brain templates from birth to adulthood. *Neuroimage* (2009) https:/doi.org/10.1016/s1053-8119(09)70884-5.

22. B. B. Avants, C. L. Epstein, M. Grossman, J. C. Gee, Symmetric diffeomorphic image registration with cross-correlation: Evaluating automated labeling of elderly and neurodegenerative brain. *Med. Image Anal.* (2008) https:/doi.org/10.1016/j.media.2007.06.004.

23. Y. Zhang, M. Brady, S. Smith, Segmentation of brain MR images through a hidden Markov random field model and the expectation-maximization algorithm. *IEEE Trans. Med. Imaging* (2001) https:/doi.org/10.1109/42.906424.

24. M. Jenkinson, P. Bannister, M. Brady, S. Smith, Improved Optimization for the Robust and Accurate Linear Registration and Motion Correction of Brain Images. *Neuroimage* **17**, 825–841 (2002).

25. D. N. Greve, B. Fischl, Accurate and robust brain image alignment using boundary-based registration. *Neuroimage* (2009) https:/doi.org/10.1016/j.neuroimage.2009.06.060.

26. Y. Behzadi, K. Restom, J. Liau, T. T. Liu, A component based noise correction method (CompCor) for BOLD and perfusion based fMRI. *Neuroimage* **37**, 90–101 (2007).

27. J. Stelzer, Y. Chen, R. Turner, Statistical inference and multiple testing correction in classification-based multi-voxel pattern analysis (MVPA): Random permutations and cluster size control. *Neuroimage* **65**, 69–82 (2013).

28. A. Abraham, *et al.*, Machine learning for neuroimaging with scikit-learn. *Front. Neuroinform.* (2014) https:/doi.org/10.3389/fninf.2014.00014.

29. T. E. J. Behrens, L. T. Hunt, M. F. S. Rushworth, The Computation of Social Behavior. *Science (80-. ).* **324**, 1160–1164 (2009).

30. R. C. Wilson, Y. Niv, Is Model Fitting Necessary for Model-Based fMRI? *PLoS Comput. Biol.* **11**, 1–21 (2015).

31. M. Lebreton, S. Bavard, J. Daunizeau, S. Palminteri, Assessing inter-individual differences with task-related functional neuroimaging. *Nat. Hum. Behav.* **3**, 897–905 (2019).

32. J. D. Power, *et al.*, Methods to detect, characterize, and remove motion artifact in resting state fMRI. *Neuroimage* (2014) https:/doi.org/10.1016/j.neuroimage.2013.08.048.

33. S. J. Gershman, N. Uchida, Believing in dopamine. *Nat. Rev. Neurosci.* **20**, 703–714 (2019).

34. T. Yarkoni, R. A. Poldrack, T. E. Nichols, D. C. Van Essen, T. D. Wager, Large-scale automated synthesis of human functional neuroimaging data. *Nat. Methods* **8**, 665–670 (2011).

35. A. G. Sanfey, J. K. Rilling, J. A. Aronson, L. E. Nystrom, J. D. Cohen, The Neural Basis of Economic Decision-Making in the Ultimatum Game. *Science (80-. ).* **300**, 1755–1758 (2003).

36. N. Kriegeskorte, R. Goebel, P. Bandettini, Information-based functional brain mapping. *Proc. Natl. Acad. Sci.* **103**, 3863–3868 (2006).

37. S. M. Smith, T. E. Nichols, Threshold-free cluster enhancement: Addressing problems of smoothing, threshold dependence and localisation in cluster inference. *Neuroimage* **44**, 83–98

(2009).